AD NUMBER

AD240188

NEW LIMITATION CHANGE

TO

Approved for public release, distribution unlimited

FROM

Distribution authorized to U.S. Gov't. agencies and their contractors; Specific Authority; 8 Jun 60. Other requests shall be referred to Naval Research Lab., Washington, DC.

AUTHORITY

Naval Research Laboratory, Technical Library, Research Reports Section Notice, dtd October 24, 2000.

NRL Report 5453

INFRARED TRANSMISSION OF THE ATMOSPHERE

H. W. Yates and J. H. Taylor

Radiometry II Branch
Optics Division

June 8, 1960

U. S. NAVAL RESEARCH LABORATORY
Washington, D.C.

NOTE

Enlarged copies of the curves shown in Figs. 5-11 will be furnished to qualified persons upon request. Address inquiries to Director, U.S. Naval Research Laboratory (Code 7360), Washington 25, D.C.

CONTENTS

Abstract	ii
Problem Status	ii
Authorization	ii
INTRODUCTION	1
INSTRUMENTATION	1
EXPERIMENTAL PROCEDURE	6
RESULTS	6
ATTENUATION BY SCATTERING	7
Introduction	7
Experimental Results	8
SELECTIVE ABSORPTION	35
Introduction	35
Atmospheric Windows	36
Experimental Results	38
ACKNOWLEDGMENTS	44
REFERENCES	45

ABSTRACT

The transmission of the atmosphere in the spectral range from 0.5 to 15 μ has been studied over three sea-level paths 0.3, 5.5, and 16.25 km in length, with an average spectral resolution, $\lambda/\Delta\lambda$, of 300. The conditions encountered covered a wide range, from 0.11 cm precipitable water in the 0.3-km path to a maximum of 33 cm precipitable water in the 16.25-km path, and values of the visual scattering coefficient were measured from 0.048 km^{-1} to 0.24 km^{-1}. Data have been evaluated on selective transmission vs water-vapor concentration for the infrared "window" regions, and the behavior of the scattering coefficient with wavelength has been plotted for representative atmospheres. Similar data were plotted for several measurements over a range of 27.7 km at an altitude of 10,000 ft.

PROBLEM STATUS

This is a final report on Problem N03-05, which was terminated Sept. 30, 1959.

AUTHORIZATION

NRL Problem N03-05
Project NO 501/825/51032/02371

Manuscript submitted January 12, 1960.

INFRARED TRANSMISSION OF THE ATMOSPHERE

INTRODUCTION

The present study was undertaken to satisfy a basic requirement in the field of military infrared technology — the measured transmission of long paths in the lower atmosphere. There have been a number of excellent direct studies of this sort in the past (1-11), but their assembled results leave a few important factors ill-defined. For one thing, the paths investigated were mostly only a few thousand yards long, the longest being three miles. Modern practice requires a knowledge of path lengths many times greater than this, and extrapolation from data on quite short paths is highly unreliable. In addition, most of the earlier experimental studies have dealt individually with either one or the other of the two major processes involved in atmospheric attenuation — selective molecular absorption by the atmospheric gases and dissipation by scattering from fog, haze, or smoke.

In order to expand the limited knowledge of atmospheric transmission, it was felt advisable to be able to measure and account for both absorption and scattering in one direct observation and to have these data apply without extrapolation to atmospheric paths of significant length. Therefore absorption spectra covering the entire practical infrared have been obtained over paths up to nearly 30 km. The instrumentation employed could not be carried to desired elevations for measurements in the upper atmosphere — certainly it was not capable of being airborne — but one path lying between two mountains about 10,000 ft above sea level was investigated in order to supply some of the information needed. The present report is the final summary of this effort. Two earlier reports have described the problem and the instrumentation and have given some of the first results (12,13). In an effort to be concise, much detail and some of the results contained in these earlier reports have not been reproduced here. It is necessary, therefore, to consider these three reports together as the final product.

INSTRUMENTATION

The three sea-level horizontal paths used in this work were of lengths 0.3, 5.5, and 16.25 km, at the Chesapeake Bay Annex (CBA) of the U.S. Naval Research Laboratory. The Annex is situated on the west shore of Chesapeake Bay near North Beach, Md. The two long paths are shown in Fig. 1. The 0.3-km path lay along the shore within the fenced area of the Annex. The measuring instruments were housed in the Optics Building at the Annex, and sources were placed at the ends of the three paths. A fourth path, 27.7 km long, lay between the mountains Mauna Loa and Mauna Kea on the Island of Hawaii. In this installation the source was located at an elevation of 9300 ft at the end of the road up Mauna Kea, while the recording instruments were housed in the U.S. Weather Bureau Station at the 11,100-ft level of Mauna Loa. Both installations were on the opposing faces of the two mountains, which are 13,784 and 13,680 ft high, respectively. Figure 2 shows the geometry of the Hawaiian path.

Note - H. W. Yates is now at Barnes Engineering Co., Stamford, Conn. J. H. Taylor is now at Southwestern University, Memphis, Tenn.

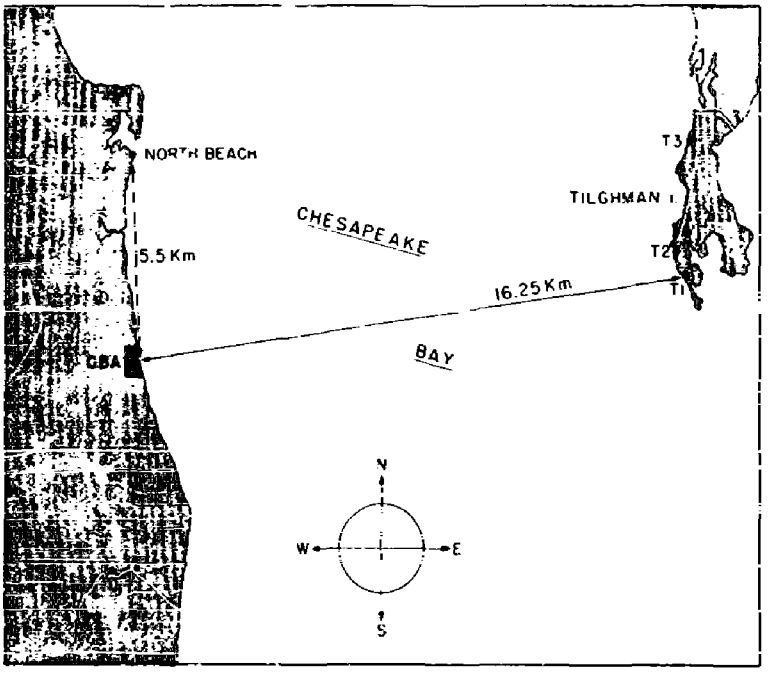

Fig. 1 - Long transmission paths in the Chesapeake Bay area

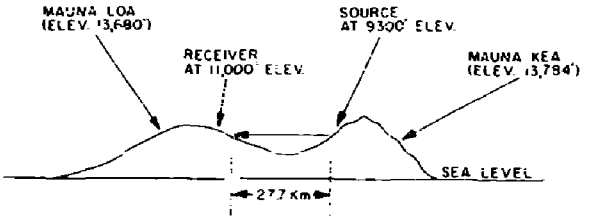

Fig. 2 - Optical-path geometry for the Hawaiian measurements

The instrumentation consisted of an unmodulated source of radiation at one end of the atmospheric path, and a monochromator with collecting mirror at the other end of the path. An auxiliary instrument was used for measuring and continuously recording the transmission of the atmosphere in the visible region of the spectrum. The sources were 60-in.-diameter carbon arc searchlights with the glass windows removed to permit operation in the infrared. With the windows removed the arc is extremely sensitive to wind, so the searchlights were placed behind baffles that acted as windshields (Fig. 3). The successful use of the carbon arc in this program required considerable care, and the interested reader is referred to the first report on this program for a detailed discussion of its operation (12). For the 0.3-km and the 5.5-km paths, one light was used as the source, for the 27.7-km path two lights were used, and for the 16.25-km path three lights were used. Multiple sources were employed both to overcome the inverse-square loss of intensity with distance and to minimize atmospheric fluctuation, or "twinkle," which usually was the limiting factor in any given measurement. By increasing the angle subtended at the collector by the source, the refractive noise, or twinkle, in the intervening atmosphere can be reduced. The rms ac noise due to twinkle has been shown to be proportional to the square root of the angle subtended by the source at the receiver (14).

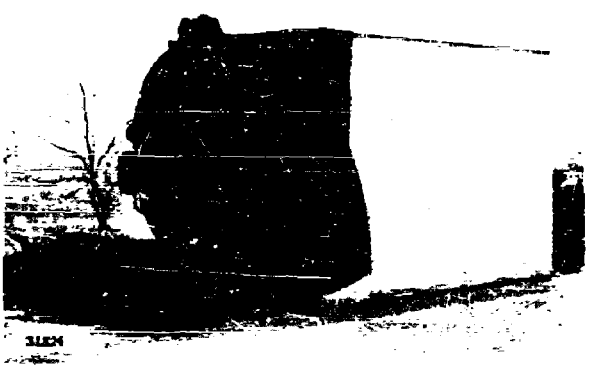

Fig. 3 - Rear view of 60-in. searchlight facing into a house-type windshield

The recording instruments used in this program were Perkin-Elmer monochromators. The installation at CBA included a Model 83 Monochromator, with LiF prism, covering the region 0.5 to 5.5 μ, and a Perkin-Elmer Model 12-C Spectrometer, with NaCl prism, covering the region 5 to 16 μ (Fig. 4). These two instruments were used simultaneously to reduce the time required for taking data and to allow the use of prisms appropriate to these two spectral regions without frequent prism changes. Frequent exposures of an NaCl prism to the air during prism changes, particularly in the atmospheres of the test areas, would result in rapid fogging and unknown changes in the spectral transmission of the instrument. Flux collection for each monochromator was accomplished by a 16-in. focal length, f/3.8 parabolic mirror arranged so that by reflection from two secondary mirrors, the images of several sources placed side by side would be rotated through 90 degrees and appear vertically along the entrance slit of the instrument (12). For the installation on Mauna Loa, one instrument was used, the Model 12-C Spectrometer, and prisms were changed to cover the full spectrum.

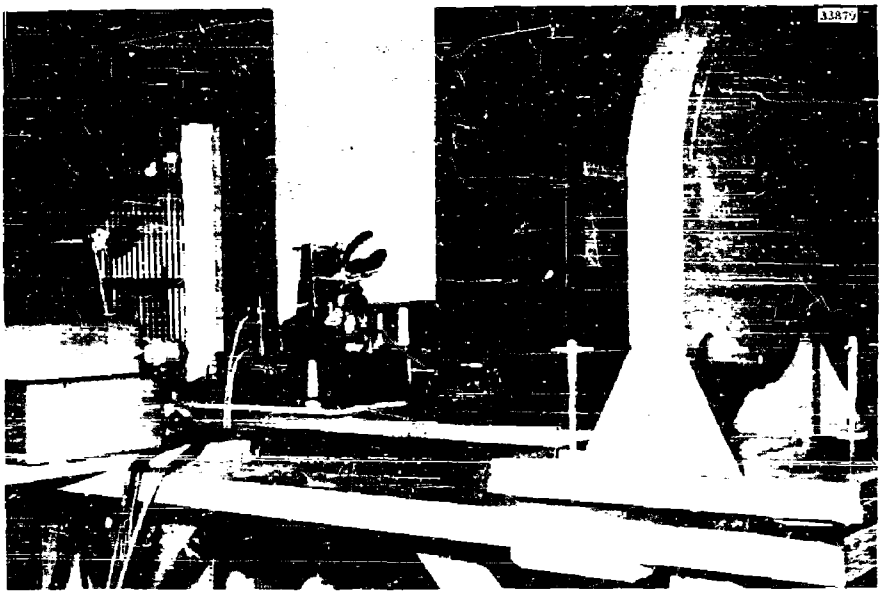

Fig. 4 - Receiver installation for the Chesapeake Bay measurements. One collector mirror is shown in the right foreground. The two monochromators with auxiliary Newtonian flats are shown center and left. One recording rack is visible in the background.

The collector mirror for the Hawaiian installation was a 24-in.-diameter, f/3.6 parabola designed for optimum use with the Perkin-Elmer instrument and manufactured by the Optical Shop, U.S. Naval Weapons Plant. The shadow of the Newtonian diagonal mirror was matched to the head of the thermocouple detector in the instrument, and the shadow of the Newtonian support rod was arranged to fall on the thermocouple support rod so that there was no loss of effective collector area. This increase in effective collector area and optical quality relative to the 16-in. collectors caused the signal level from two lights over the 27.7-km path in Hawaii to be only moderately less than the signal from three lights over the 16.25-km path at CBA. The use of only two lights in the Hawaiian installation was the result of logistic limitations. The installation and maintenance of such large equipments in difficult areas are formidable problems.

The radiation detectors were Perkin-Elmer thermocouples. The outputs from the thermocouples were amplified by Perkin-Elmer 13-cps breaker amplifiers and recorded on Speedomax Type G recorders. Wavelength calibration was carried out on the spectrometers at all installations by using the emission of a General Electric H-4 mercury lamp and the absorption bands of H_2O, CO, CO_2, CH_4, HCl, HBr, and CH_3OH. Wavelengths for this calibration were taken from Ref. 15.

In Hawaii, the transmission in the visible region of the spectrum was determined by observing a calibrated lamp with a visual telephotometer. The telephotometer is of the low-brightness Rochester type and must be used at night (16). Therefore, operation at the Hawaii site was limited to night, when measurements of the visual transmission could be made before and after a transmission spectrum was taken. At CBA, two recording transmissometers were installed, and they continuously recorded the visual transmission over the 5.5- and 16.25-km paths by day and night so that infrared transmission spectra could be measured at any time. These transmissometers are linear recording instruments that require nighttime calibration by the low-brightness telephotometer (16).

Conventional use of the low-brightness telephotometer requires the use of a calibrated lamp and absolute calibration of the telephotometer. The lamp is placed at one end of the path to be measured, and the illumination produced at the other end of the path is measured with the telephotometer. Any reduction below that calculated from inverse-square loss is attributed to the losses in the atmosphere. These quantities are related by the following equation:

$$R = K \frac{I}{D^2} T, \tag{1}$$

where

R = telephotometer reading (arbitrary divisions)

K = calibration constant of photometer (ft-candles/division)

I = intensity of lamp (candlepower)

D = path length (ft)

T = transmission of the atmosphere over path length D.

The technique used in the present program takes advantage of the fact that transmission is a dimensionless number requiring absolute calibration of neither the lamp nor the telephotometer. A calibration of the telephotometer relative to a given large lamp is carried out by using a small intermediary lamp to simulate at short distance the effect of the large lamp at great distances. This small lamp (about 1 candlepower) is placed about 150 ft from the telephotometer, and greater distances up to 1500 ft are simulated by whirling sector discs in front of the lamp. The telephotometer readings are then given by

$$R = K \frac{i}{d^2} t, \tag{2}$$

where

i = intensity of the small lamp (candlepower)

d = effective distance (increased by sector discs) between telephotometer and lamp (ft)

t = transmission of 150-ft path used.

If R is adjusted to be the same for both the large distant lamp and the small lamp, Eqs. (1) and (2) can be equated.

$$\frac{I}{D^2} T = \frac{i}{d^2} t, \tag{3}$$

with K dropping out. Over the short 150-ft path, t can be considered to be 100 percent, so that

$$T = \left(\frac{i}{I}\right)\left(\frac{D^2}{d^2}\right). \tag{4}$$

It is therefore necessary only to know the intensity ratio (i/I) for the two lamps and the two distances d and D. The large lamps used were 1000-watt airway beacon lamps of

about 1500 candlepower, and the intensity ratios between them and the small 1-candlepower lamps were obtained on a photometry bench, where one leg was about 130 ft.

Measuring d for each individual transmission measurement was not practical in the field, and so the telephotometer was calibrated in terms of $1/d^2$ for one particular small lamp. Thus, when a measurement was made over a particular path of known length D, the telephotometer was used to measure a value of $1/d^2$ for the large remote lamp, and transmission was calculated from D, $1/d^2$, and the previously measured intensity ratio (i/I).

EXPERIMENTAL PROCEDURE

The first step in the measurement of the infrared transmission of the atmosphere was to measure the radiation from the source over the 0.3-km path. It was felt that a satisfactory vacuum envelope could be drawn from such a spectrum. The LiF instrument scanned the spectral region from 0.5 to 5.2 μ, and the NaCl instrument scanned the region from 2.72 to 15 μ. In recording the spectrum over the 0.3-km path, maximum resolution was not used. Instead, a slit schedule was used which would give sufficient signal when used with the longest paths. The choice of a 0.3-km reference path, rather than a much shorter one, was made primarily to make the geometry approach that which existed in the case of the distant lights. In all cases, it was the searchlight mirror which was imaged on the entrance slits. The vacuum envelope used in reducing the data was obtained from several runs made on the 0.3-km path. All of these runs were reproducible to about two percent.

The second step in the procedure was to record the infrared spectrum over one of the distant paths with the same slit program used in the 0.3-km path. By taking the ratio of the deflection at a given wavelength obtained over the distant path to the deflection obtained over the 0.3-km path, a number proportional to transmission was obtained. Since absolute transmission values were required, it was necessary to determine a factor which, when multiplied by the above-mentioned ratio, would yield the absolute transmission at the given wavelength. This factor was determined at 0.55 μ for each path by means of the visual telephotometer and auxiliary light source.

When the factor at 0.55 μ which would yield absolute transmission values was determined, the spectrum obtained with the LiF instrument was then reduced point by point to absolute transmission values. A plot was then made of transmission versus wavelength from 0.55 to 5.2 μ. Since the region from 2.72 to 4.2 μ was scanned by both the LiF and NaCl instruments, it was used as a tie-down region for the normalization of the NaCl measurements. For this region, the area under the curve obtained with the LiF instrument was planimetered, and an average absolute transmission was calculated. The same procedure was repeated for this window using the spectrum obtained with the NaCl instrument. The value obtained was proportional to the average absolute transmission in the window. It was then possible to calculate the factor which, when multiplied by the average value obtained with the NaCl instrument, would yield the average absolute transmission as obtained with the LiF instrument. Knowing this factor, it was possible to reduce point by point the spectrum obtained with the NaCl instrument in the long-wavelength region to absolute transmission values.

RESULTS

The basic data on which the results of this report are based consist of 51 complete spectra covering the region 0.5 to 15 μ with an average resolution, $\lambda/\Delta\lambda$, of about 300. Of the 51 complete spectra, 15 were reduced to absolute values of transmission vs wavelength over the full spectral range, five more were reduced only to values of scattering

coefficient vs wavelength, and five others were reduced only to values of selective window transmission vs water-vapor content. The remaining 26 were found, upon examination, to duplicate the conditions and results of spectra already reduced. Except for a cursory check sufficient to establish the degree of agreement (±5 percent for selective window transmission and ±10 percent for scattering coefficient is the average agreement found between any two runs covering near-identical conditions), nothing further has been done to these spectra. They are all on file at the U.S. Naval Research Laboratory in the form of unreduced Speedomax chart records.

Nine of the complete spectra, selected to be representative samples of the total number, are reproduced in Figs. 5 through 10. One additional spectrum (Fig. 11) was recorded for a short path under maximum resolution with the prism spectrometer by using LiF, CaF, NaCl, and KBr prisms to cover the interval from 0.5 to 26 μ with a resolution ranging from 1 to 2 wave numbers in the region beyond 2 μ. Another set of three spectra, one each over the 0.3-, 5.5-, and 16.25-km paths, was published in an earlier report (12) and is not included here. A wide range of precipitable water is represented — from 0.11 cm in the 0.3-km path to a maximum of 38 cm in the 16.25-km path — and values of the visual scattering coefficient range from 0.048 km^{-1} to 0.24 km^{-1}.

ATTENUATION BY SCATTERING

Introduction

Scattering accounts for a significant loss of flux from any collimated or narrow light beam passing through the atmosphere. The molecules of air scatter light, but their effect is negligible in the infrared, which is the region of the spectrum considered here. Although some solid matter is suspended in the air and contributes to the scattering, it is primarily droplets of liquid water, deposited on condensation nuclei, that account for most of the scattering in the atmosphere. Arid regions are always known for atmospheric clarity and humid regions for haze and fog. A short atmospheric path on the east coast contains sufficient haze to give a milky appearance to the terrain beyond, while the Rocky Mountains are usually visible for a hundred miles or more.

The scattering properties of the atmosphere are most frequently described by the scattering coefficient σ, which gives the flux scattered into 4π steradians from a unit volume of air irradiated by parallel light producing unit irradiance at the unit volume. The transmission t of a purely scattering path of length x for parallel radiation is related to the scattering coefficient by the expression

$$t = e^{-\sigma x},$$

where the assumption is that σ does not vary along the path.

Most generally, the quantity σ is a function of wavelength and is properly defined only by reference to the spectral distribution of the light. In this report it is defined for monochromatic light and should be called the monochromatic scattering coefficient. For convenience the shorter term is used.

The variation of σ with wavelength was one of the areas of interest in the present work, and it is appropriate to review briefly the parameters which determine the variation. The theory of light scattering by dielectric particles predicts that σ is defined by the following expression:

$$\sigma = \sum_{N} 2\pi K \left(\frac{r}{\lambda}\right) r^2 N, \qquad (5)$$

where N is the concentration of particles with radius r, K is a function of the quantity r/λ and the refractive index of the particle, and λ is the wavelength. The quantity $K(r/\lambda)$ can be computed theoretically.

The key parameter is the quantity r/λ, the dimension of the particle relative to the wavelength. For $r/\lambda \ll 1$, σ varies as $1/\lambda^4$ (Rayleigh scattering). For $r/\lambda \gg 1$, σ is independent of λ, and the scattering is nonselective. The intermediate case $r \propto \lambda$ is called Mie scattering and is theoretically the most complex case. In any real atmosphere there is a wide distribution of particle sizes, and the scattering coefficient at a particular wavelength is determined by summing over the whole size range.

The present data were used to estimate typical values of σ as a function of wavelength for real atmospheres. There are very few published data for this type of function through the near infrared, yet the information is quite necessary to estimate transmission over long paths.

The present work deals with real atmospheres, and in any work of this type it is convenient to characterize an atmosphere by indicating its transmittance for visible light. Frequently this is expressed as a "visibility," or the distance at which a large black object can just be detected against the horizon. This concept, however, involves the variable contrast threshold of the human eye and is not a satisfactory one. A sort of idealized "visibility" is preferable, and this has been termed Meteorological Range (MR). This is the length of air path in which the scattered light produces a luminance equal to 98 percent of the luminance of an infinitely long airpath of the same characteristics. The contrast of a dark object against the horizon is thus reduced to 2 percent if the object is at the MR. Although the concept involves white light and the standard curve of human vision, it can also be applied to monochromatic light at 5500 A, and is so applied here. The MR is related to the scattering coefficient σ by the relation

$$MR = \frac{3.94}{\sigma}.$$

Figure 12 shows a plot of MR vs scattering coefficient. Also shown in Fig. 16 as a series of solid points are values of visual range vs scattering coefficient, as derived from the International Visibility Tables. The two sets of values differ slightly because the contrast threshold of the human eye, which enters into the visibility criteria, differs somewhat from the 2-percent threshold assumed for the MR.

Experimental Results

Scattering coefficients, σ/km, were determined at 12 wavelengths from 14 of the most reliable spectra. The determination was based on the assumption that absorption is negligible at certain spectral points away from intense absorption bands, and that in these "windows" the measured attenuation could be completely attributed to scattering. This assumption appears quite valid for the wavelengths 0.55, 0.60, 0.70, 0.80, 0.90, 1.06, 1.26, 1.67, 2.17, 3.5, and 4.0 μ, and σ was computed for these points. Values of σ were also computed for 4.70 μ, even though the assumption is not valid at this wavelength because of the presence of weak absorption bands throughout the "window." The assumption is also generally invalid at longer wavelengths. It is possible that with very high resolution small regions free of absorption could be found at longer wavelengths, but none were discernible in this work.

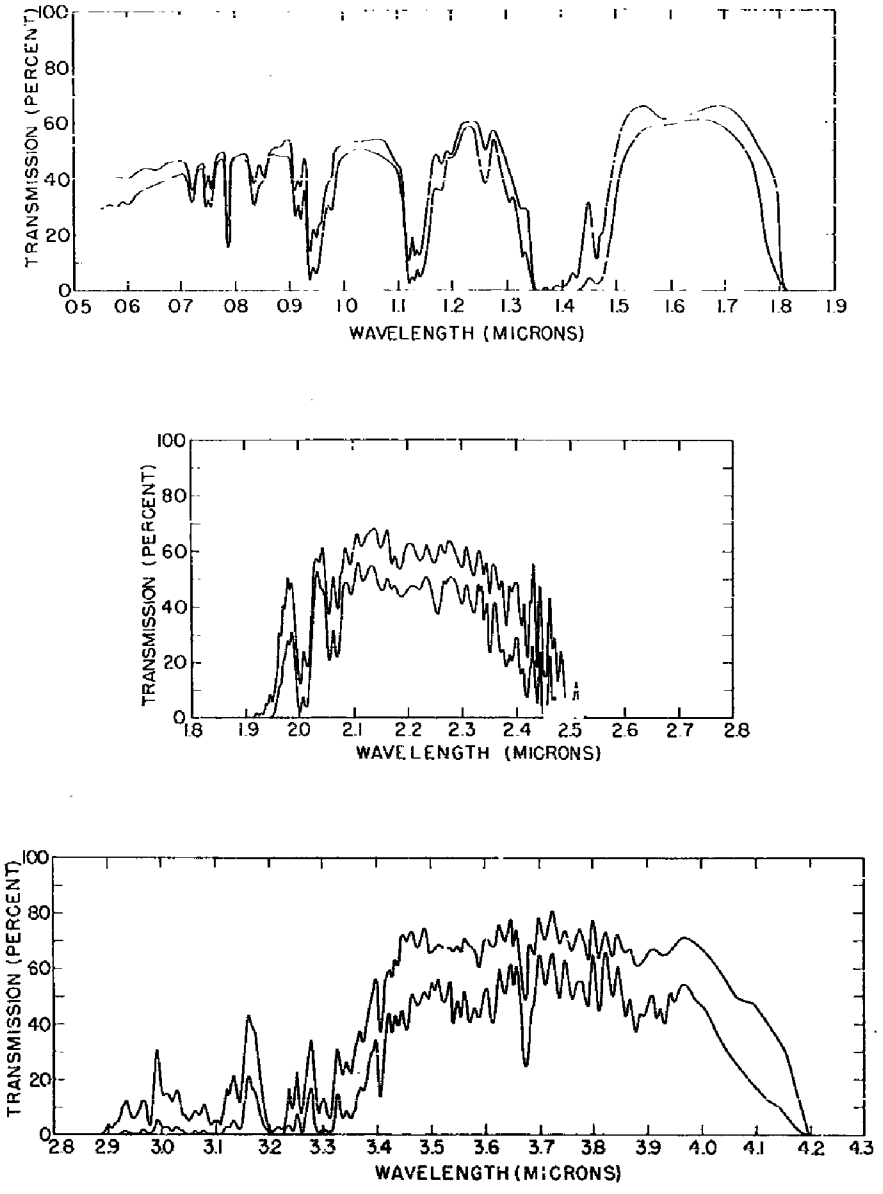

Fig. 5 - Atmospheric transmission over 5.5 km and 16.25 km in the Chesapeake Bay area. Data from runs 58 and 60 over 5.5 km and from runs 59 and 61 over 16.25 km.

5.5 km – April 19, 1956, 38°F, 66 percent R.H.,
2.2 cm H_2O in path, 40 percent transmission at 0.55 μ

16.25 km – April 19, 1956, 53°F, 41 percent R.H.,
6.5-6.9 cm H_2O in path, 29 percent transmission at 0.55 μ

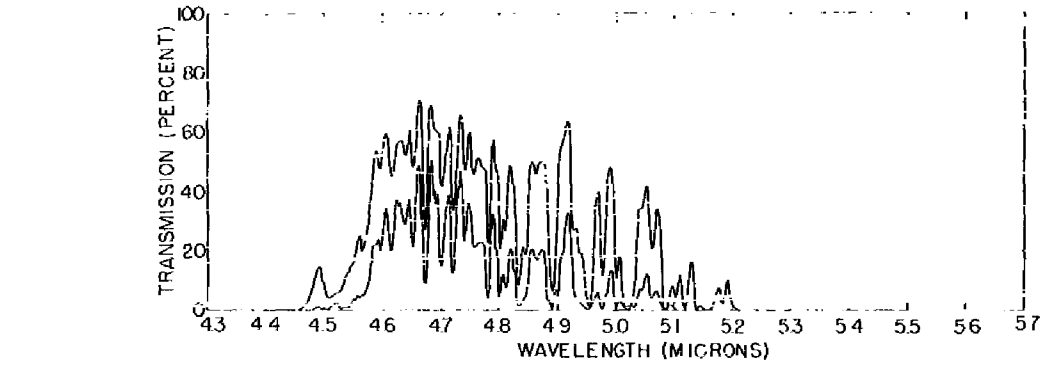

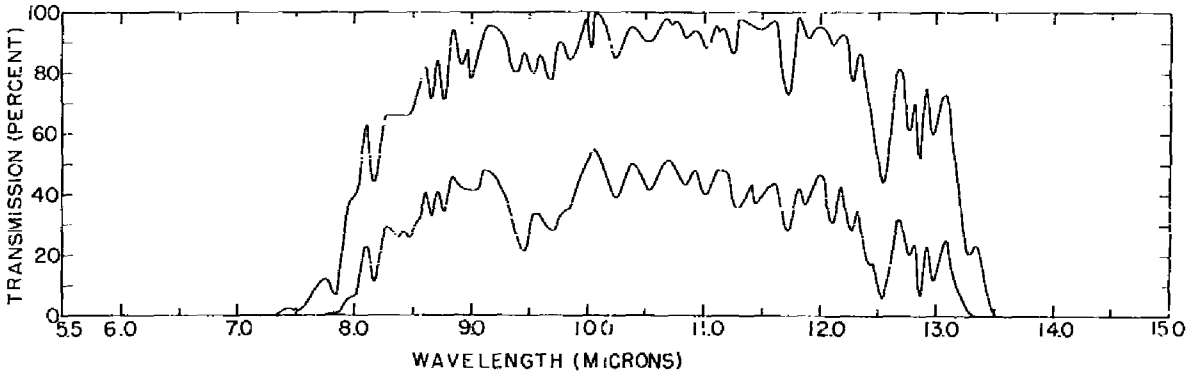

Fig. 5 (Continued) - Atmospheric transmission over 5.5 km and 16.25 km in the Chesapeake Bay area. Data from runs 58 and 60 over 5.5 km and from runs 59 and 61 over 16.25 km.

5.5 km - April 19, 1956, 38°F, 66 percent R.H.,
2.2 cm H_2O in path, 40 percent transmission at 0.55 μ

16.25 km - April 19, 1956, 53°F, 41 percent R.H.,
6.5-6.9 cm H_2O in path, 29 percent transmission at 0.55 μ

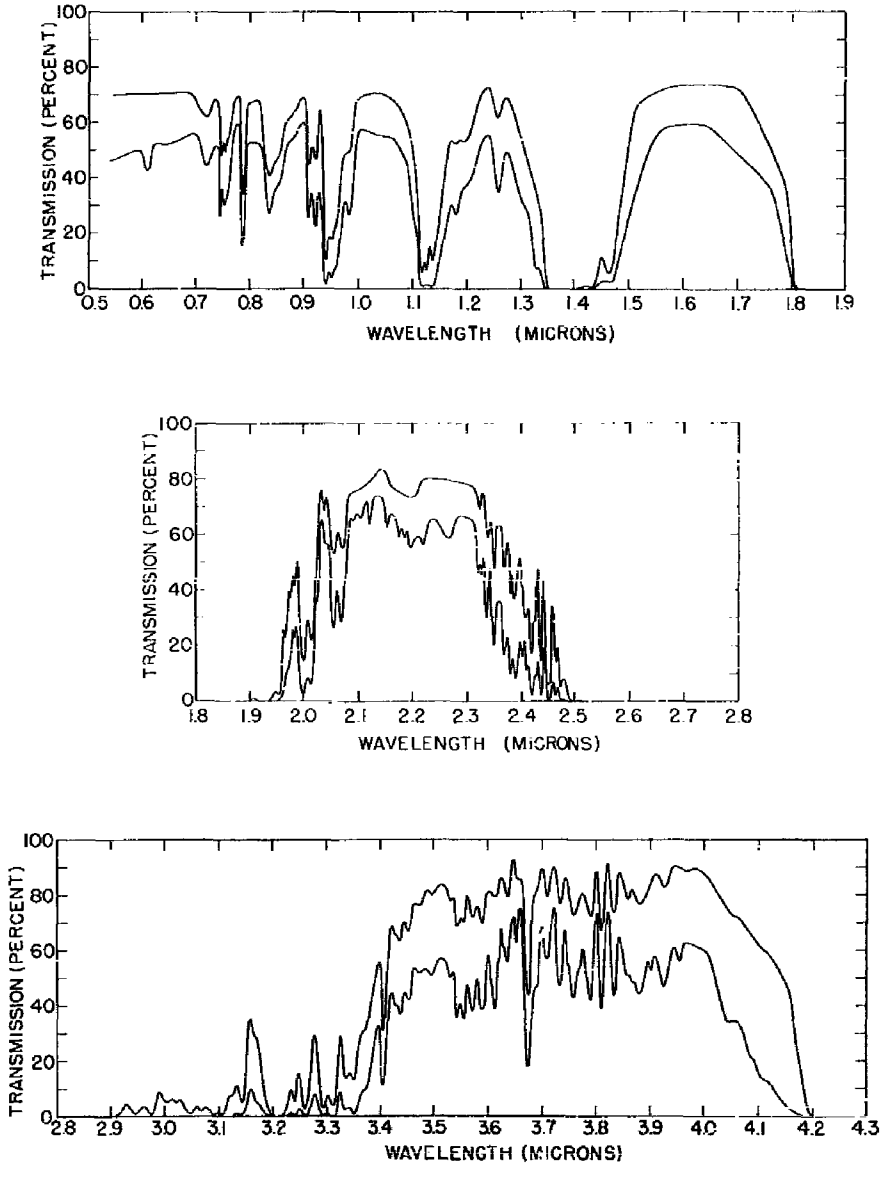

Fig. 6 - Atmospheric transmission over 5.5 km and 16.25 km in the Chesapeake Bay area. Data from runs 70 and 71 over 5.5 km and from runs 68 and 69 over 16.25 km.

5.5 km - June 19, 1956, 9 p.m., 64°F, 51 percent R.H., 4.18 cm H_2O in path, 70 percent transmission at 0.55 μ

16.25 km - June 19, 1956, 4 p.m., 68.7° F, 53 percent R.H., 15.1 cm H_2O in path, 43 percent transmission at 0.55 μ

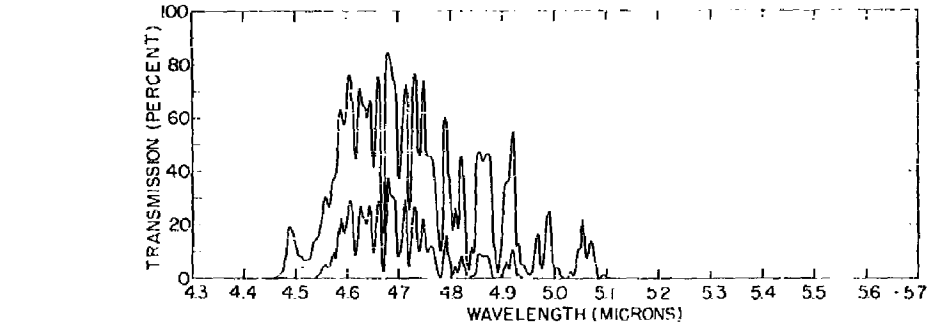

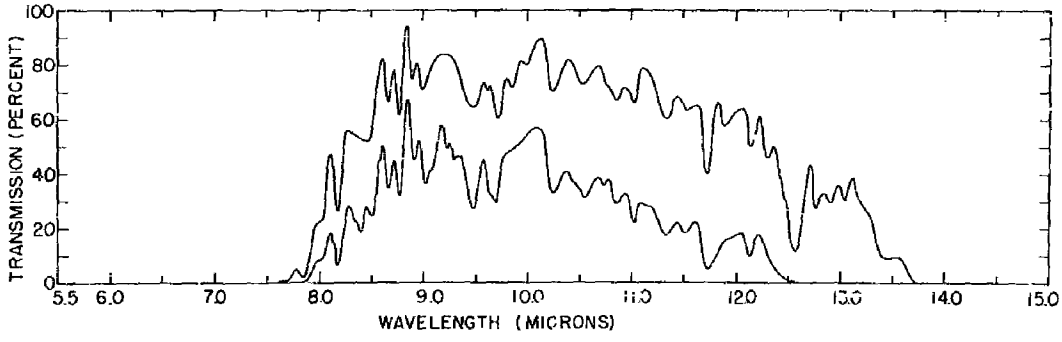

Fig. 6 (Continued) - Atmospheric transmission over 5.5 km and 16.25 km in the Chesapeake Bay area. Data from runs 70 and 71 over 5.5 km and from runs 68 and 69 over 16.25 km.

5.5 km – June 19, 1956, 9 p.m., 64°F, 51 percent R.H., 4.18 cm H_2O in path, 70 percent transmission at 0.55 μ

16.25 km – June 19, 1956, 4 p.m., 68.7°F, 53 percent R.H., 15.1 cm H_2O in path, 43 percent transmission at 0.55 μ

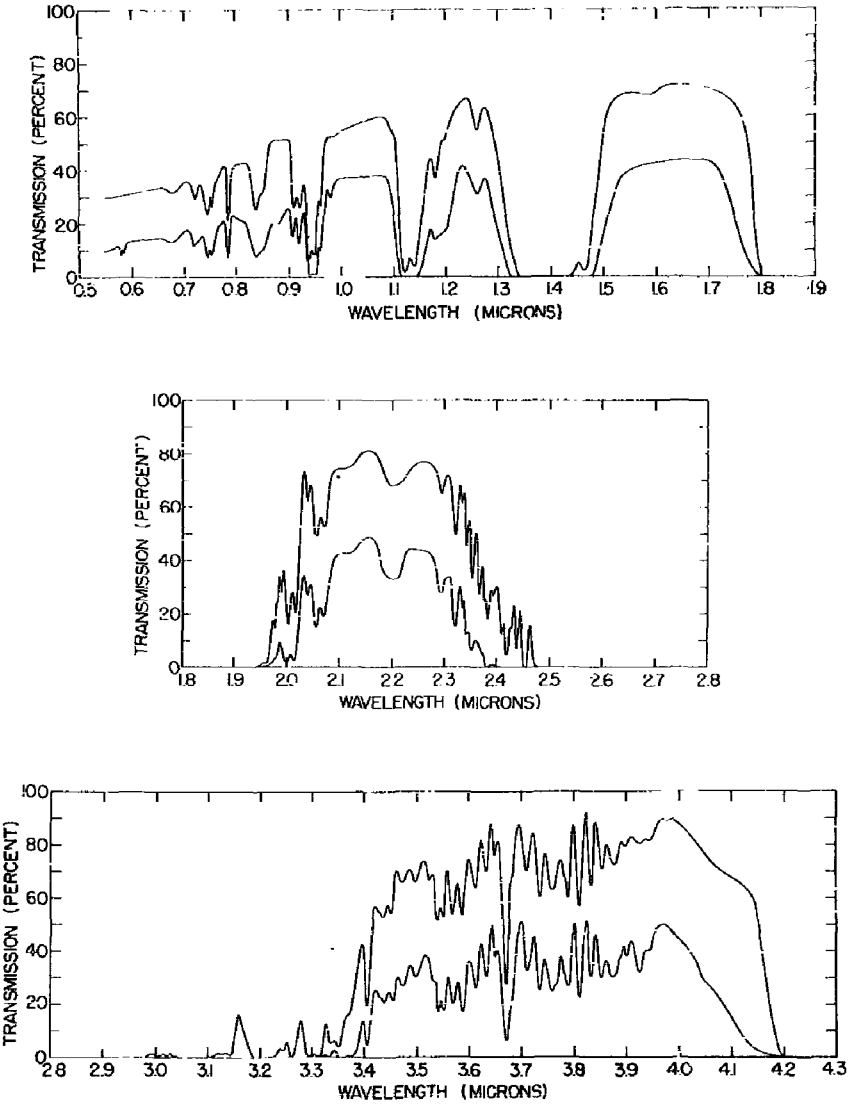

Fig. 7 - Atmospheric transmission over 5.5 km and 16.25 km in the Chesapeake Bay area. Data from runs 78 and 81 over 5.5-km path, and from runs 77 and 80 over 16.25 km.

5.5 km - Aug. 27, 1956, 6 p.m., 78°F, 73 percent R.H., 9.4 cm H_2O in path, 30 percent transmission at 0.55 μ

16.25 km - Aug. 27, 1956, 11 a.m., 74°F, 82 percent R.H., 27.7 cm H_2O in path, 10 percent transmission at 0.55 μ

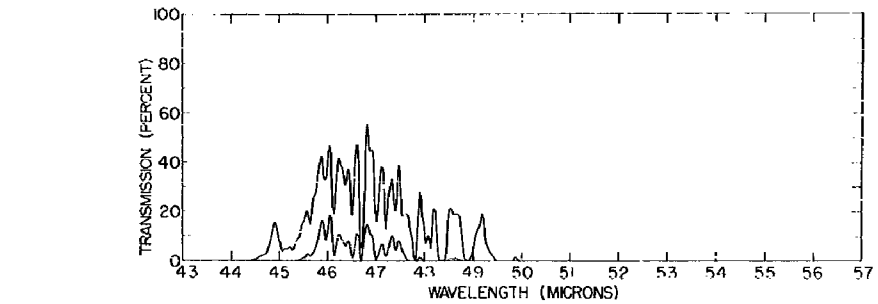

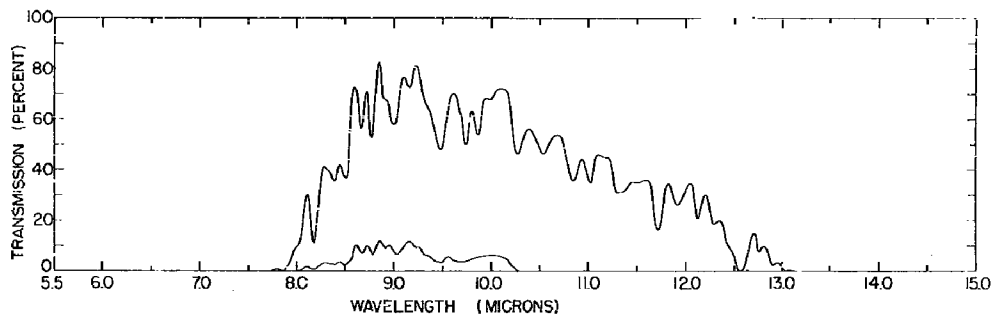

Fig. 7 (Continued) – Atmospheric transmission over 5.5 km and 16.25 km in the Chesapeake Bay area. Data from runs 78 and 81 over 5.5-km path, and from runs 77 and 80 over 16.25 km.

5.5 km – Aug. 27, 1956, 6 p.m., 78°F, 73 percent R.H., 9.4 cm H_2O in path, 30 percent transmission at 0.55 μ

16.25 km – Aug. 27, 1956, 11 a.m., 74°F, 82 percent R.H., 27.7 cm H_2O in path, 10 percent transmission at 0.55 μ

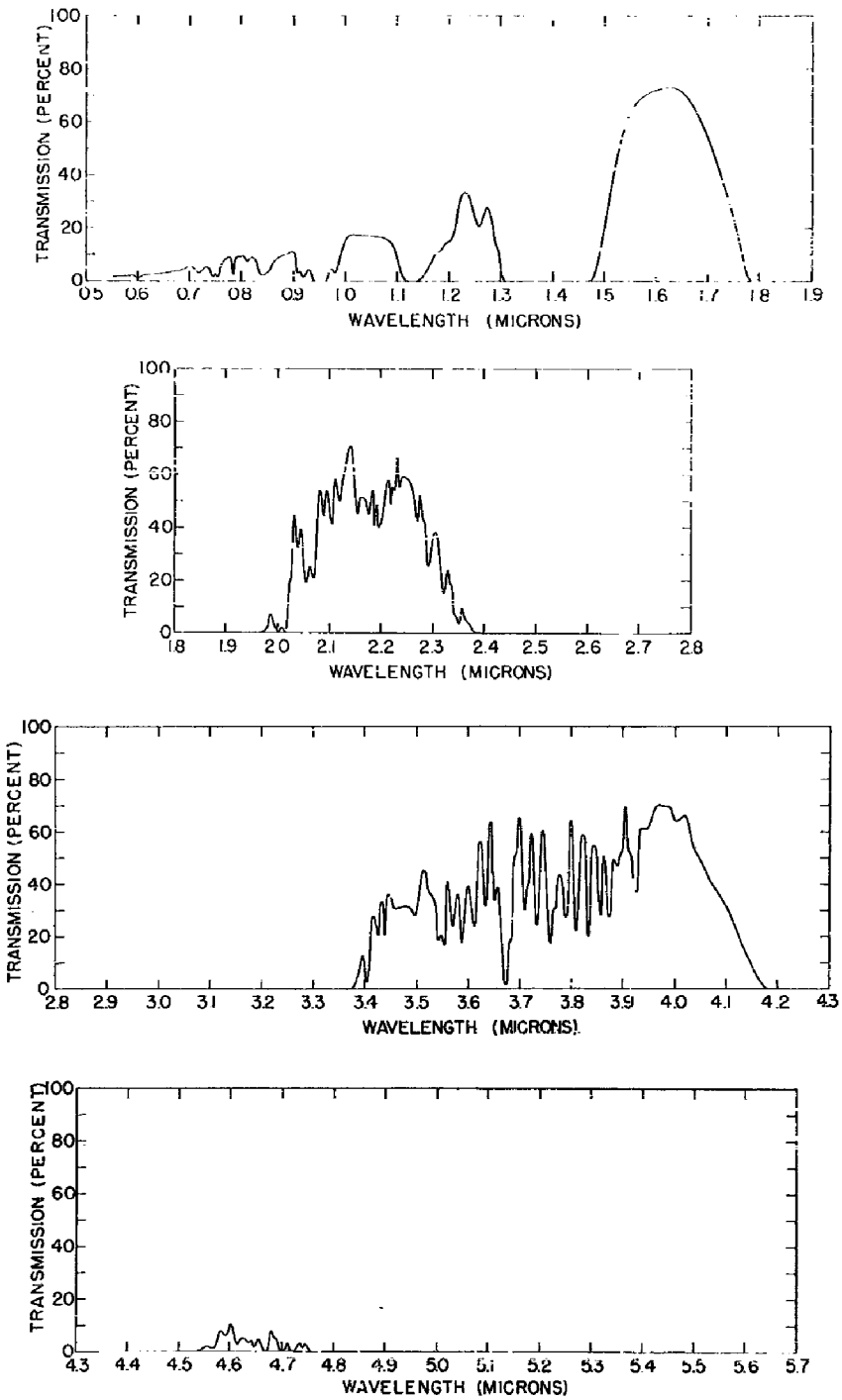

Fig. 8 - Atmospheric transmission over 16.25-km path in the Chesapeake Bay area. Data from run 83.

16.25 km - June 16, 1957, 7 p.m., 87.5°F, 59 percent R.H., 36-38 cm H_2O in path, 2 percent transmission at 0.55 μ

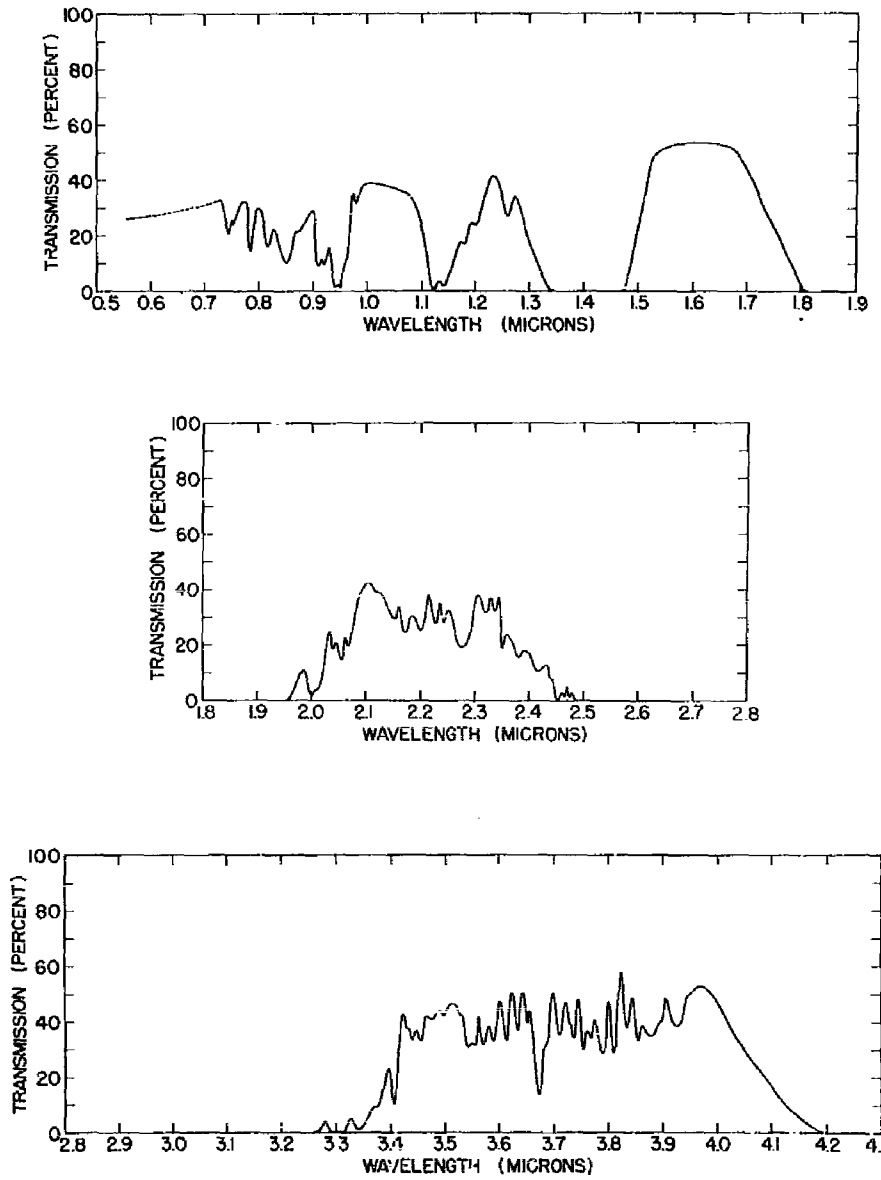

Fig. 9 - Atmospheric transmission over 27.7 km in the Hawaiian Islands. Data from run ML-3.

27.7 km - 10,000-ft altitude, Sept. 1, 1957, 11:30 a.m., 43°F, 100 percent R.H., 20 cm H_2O in path, 26.5 percent transmission at 0.55 μ

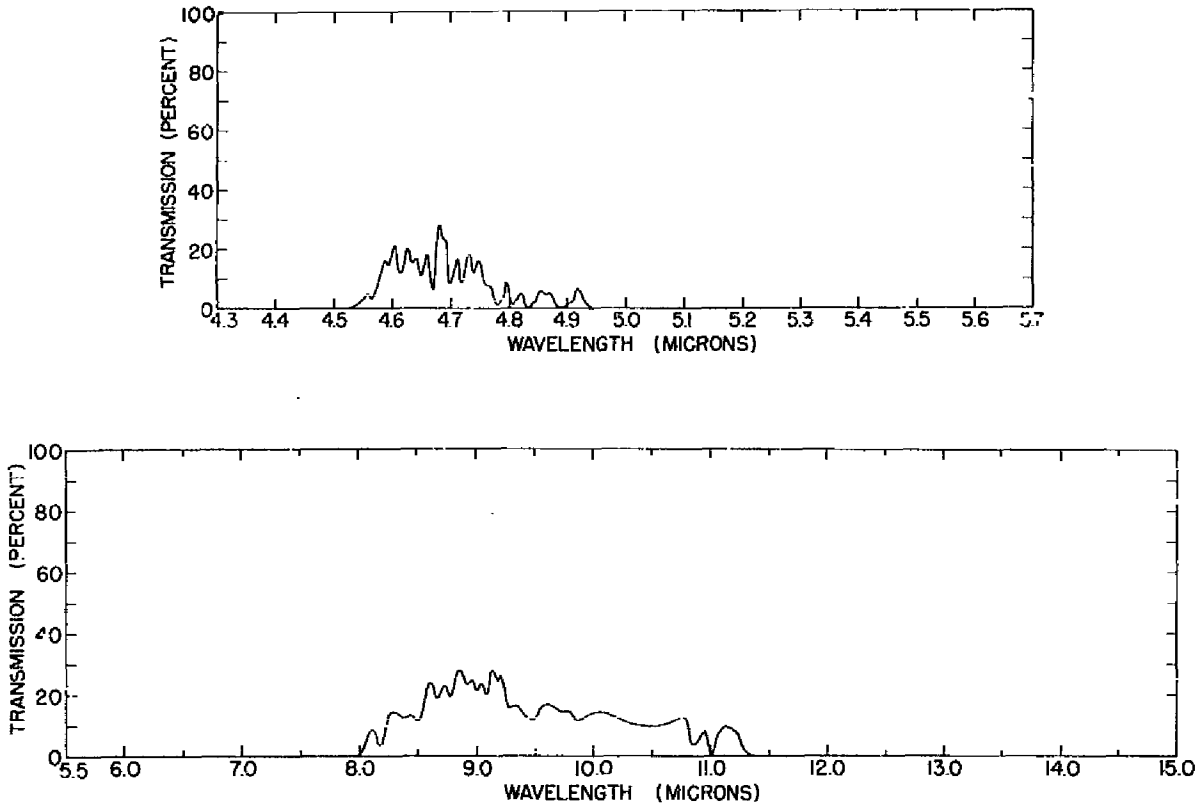

Fig. 9 (Continued) - Atmospheric transmission over 27.7 km in the Hawaiian Islands. Data from run ML-3.

27.7 km - 10,000-ft altitude, Sept. 1, 1957, 11:30 a.m., 43°F, 100 percent R.H., 20 cm H_2O in path, 26.5 percent transmission at 0.55 μ

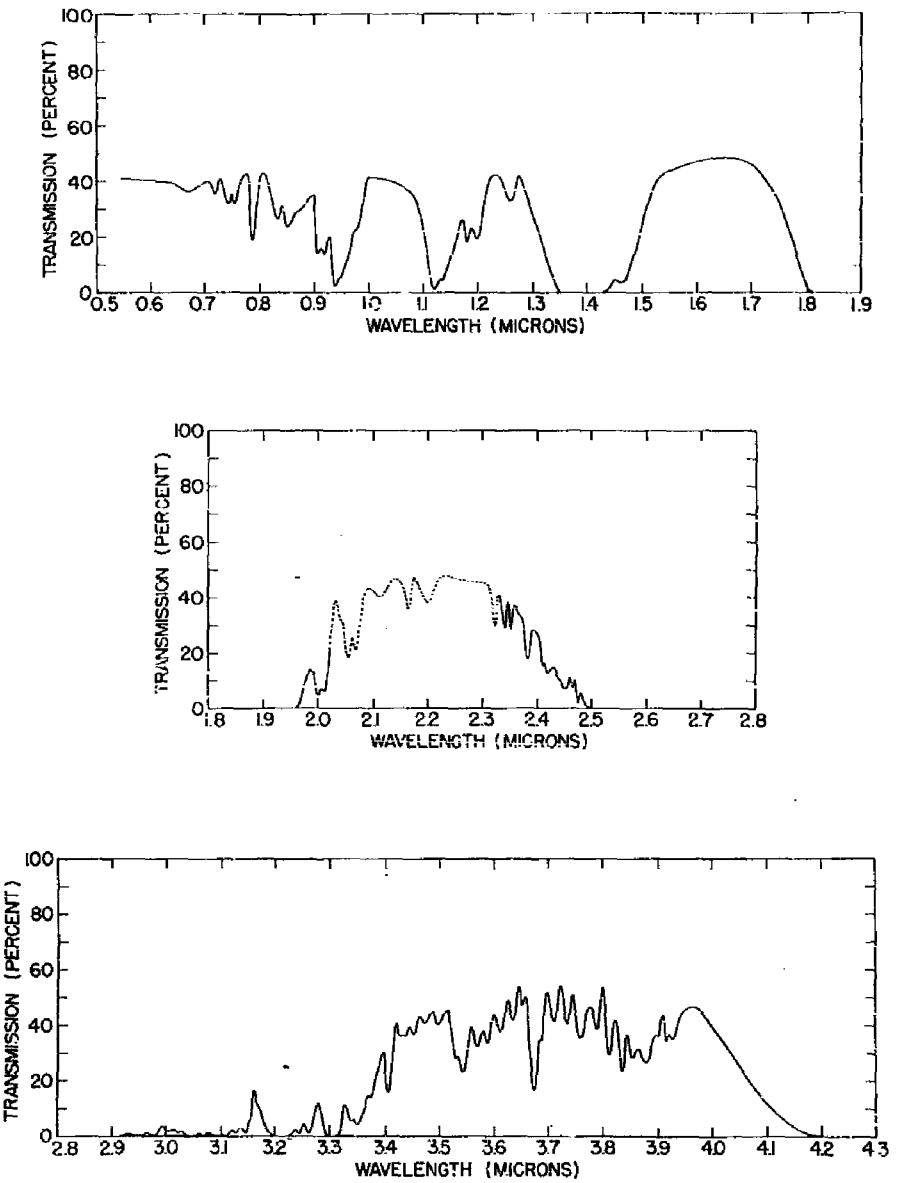

Fig. 10 - Atmospheric transmission over 27.7 km in the Hawaiian Islands. Data from run ML-6.

27.7 km - 10,000-ft altitude, Sept. 6-7, 1957, 11:00 p.m., 8-13 cm H_2O in path, 41 percent transmission at 0.55 μ

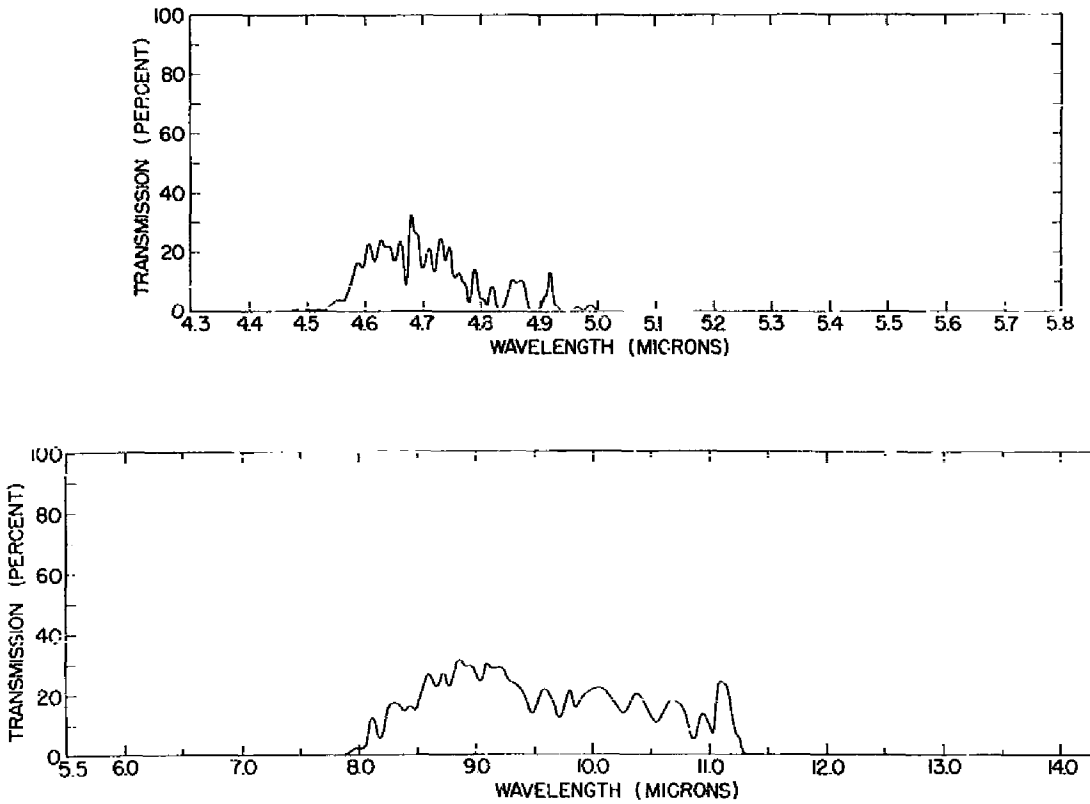

Fig. 10 (Continued) - Atmospheric transmission over 27.7 km in the Hawaiian Islands. Data from run ML-6.

27.7 km - 10,000-ft altitude, Sept. 6-7, 1957, 11:00 p.m., 8-13 cm H_2O in path, 41 percent transmission at 0.55 μ

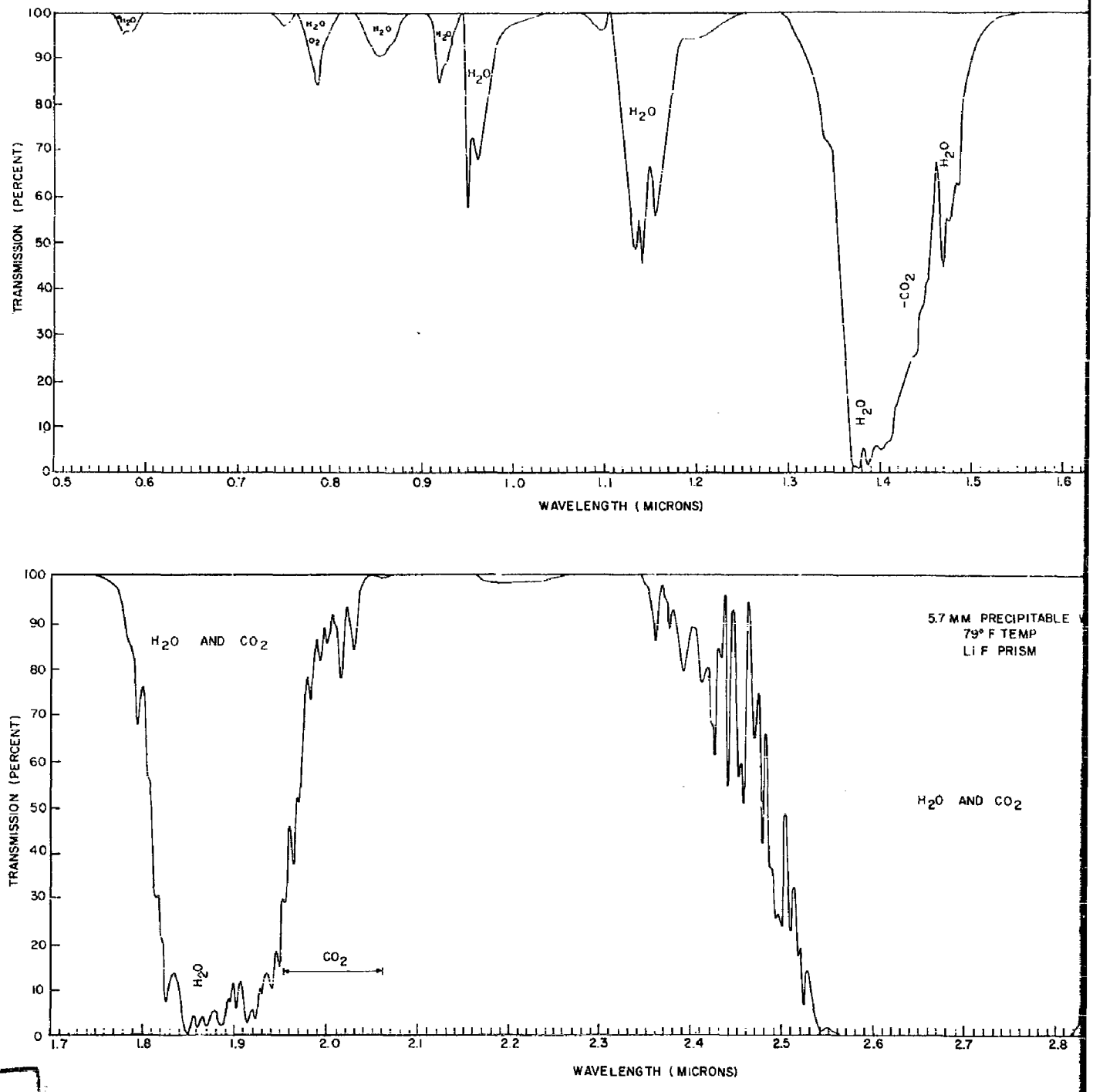

Fig. 11 - Atmospheric transmission over a 0.3-km path in the Chesapeake Bay area. Maximum available resolution used.

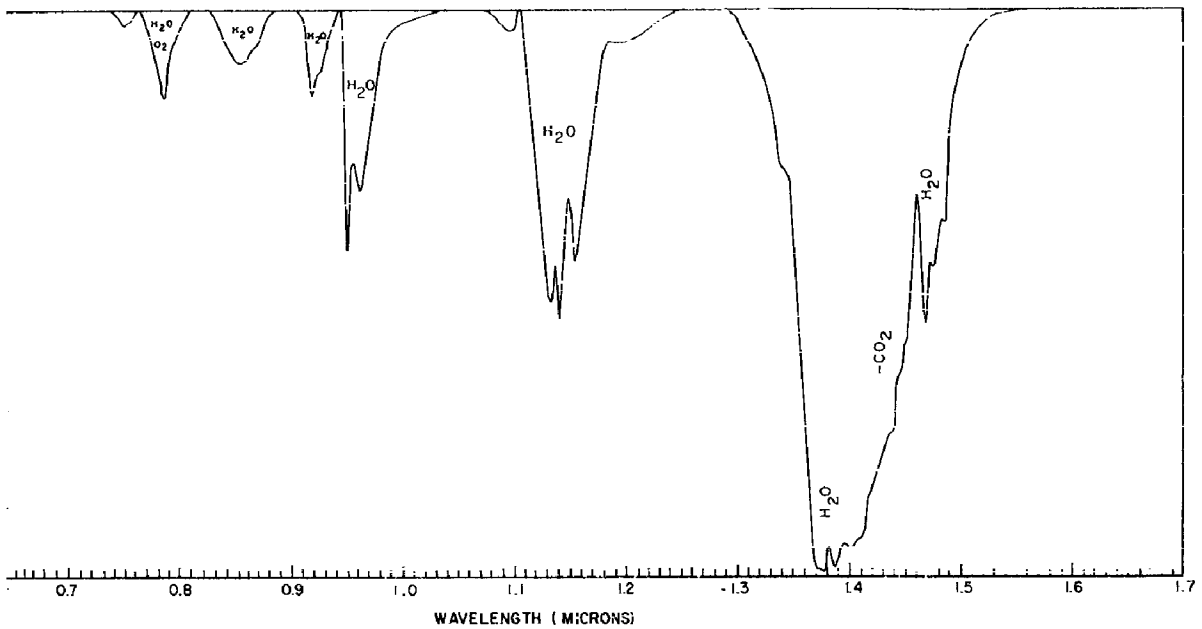

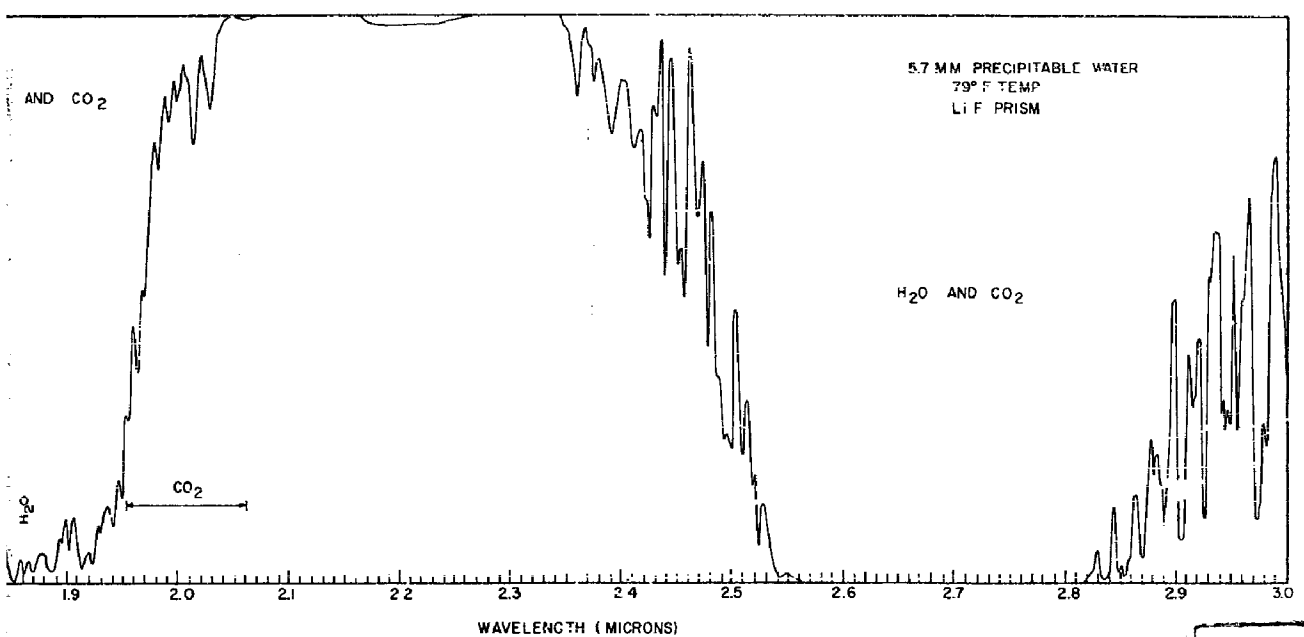

Fig. 11 - Atmospheric transmission over a 0.3-km path in the Chesapeake Bay area. Maximum available resolution used.

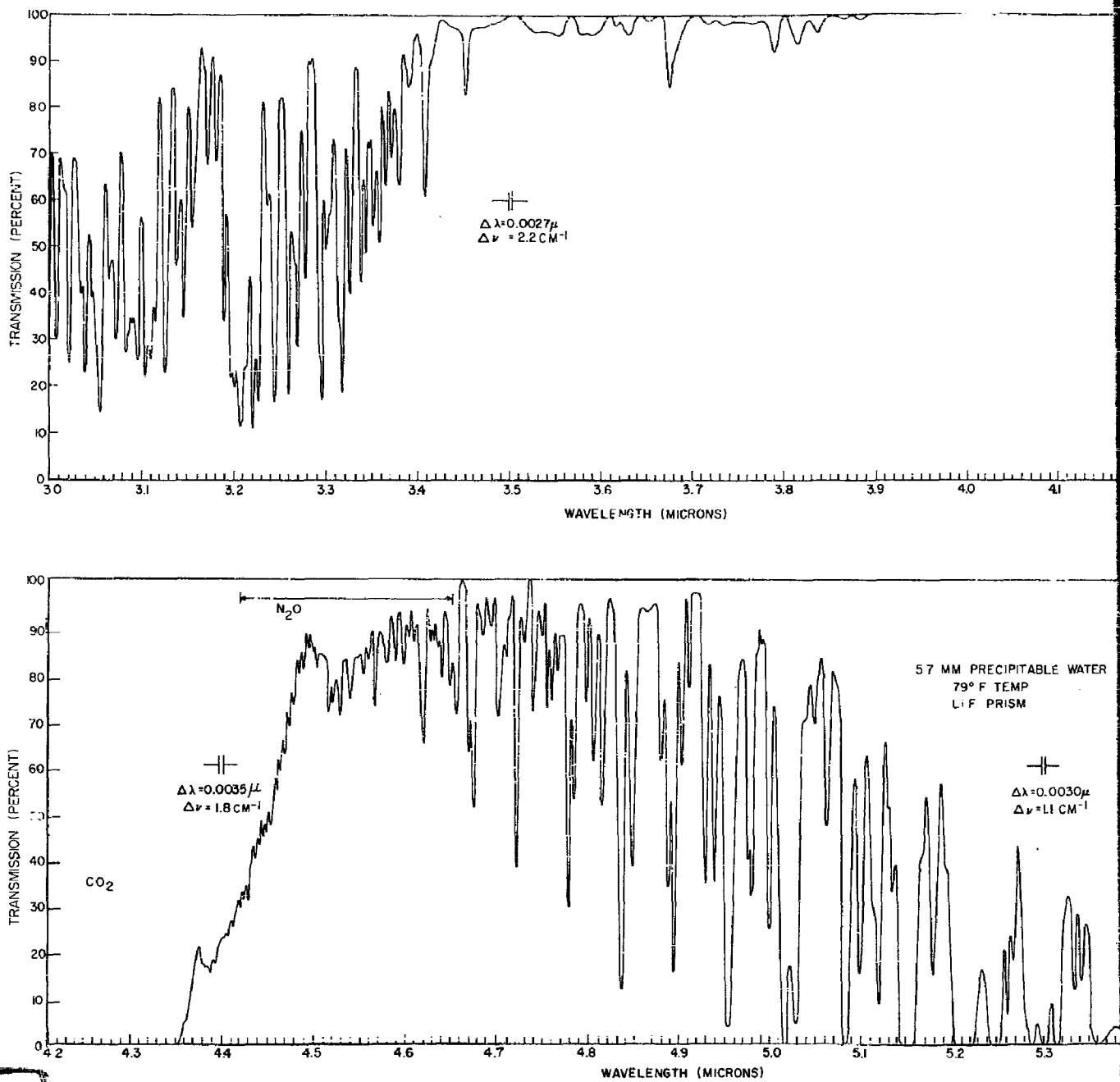

Fig. 11 (Continued) - Atmospheric transmission over a 0.3-km path in the Chesapeake Bay area. Maximum available resolution used.

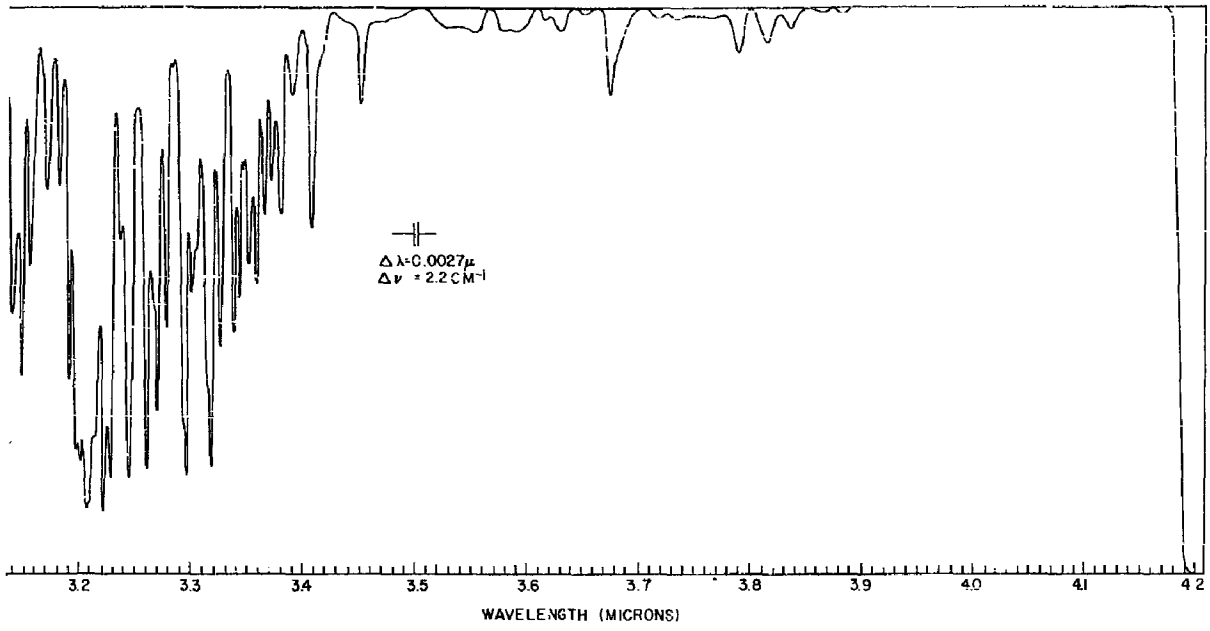

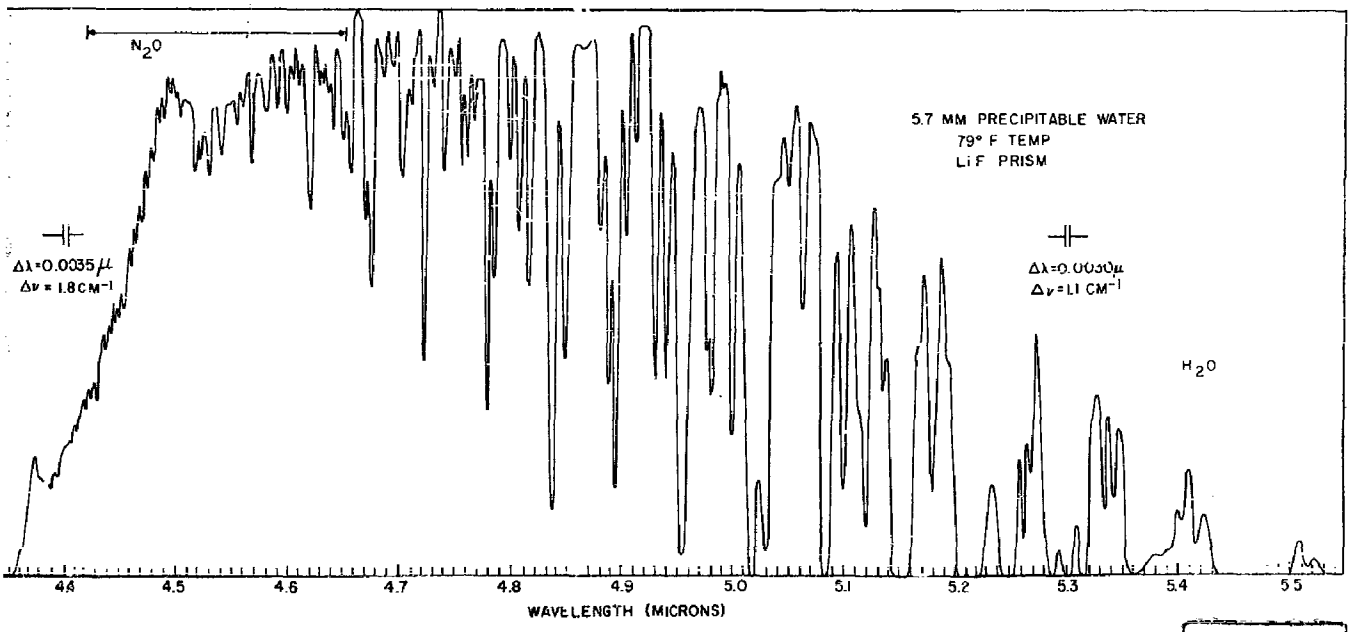

Fig. 11 (Continued) - Atmospheric transmission over a 0.3-km path in the Chesapeake Bay area. Maximum available resolution used.

2

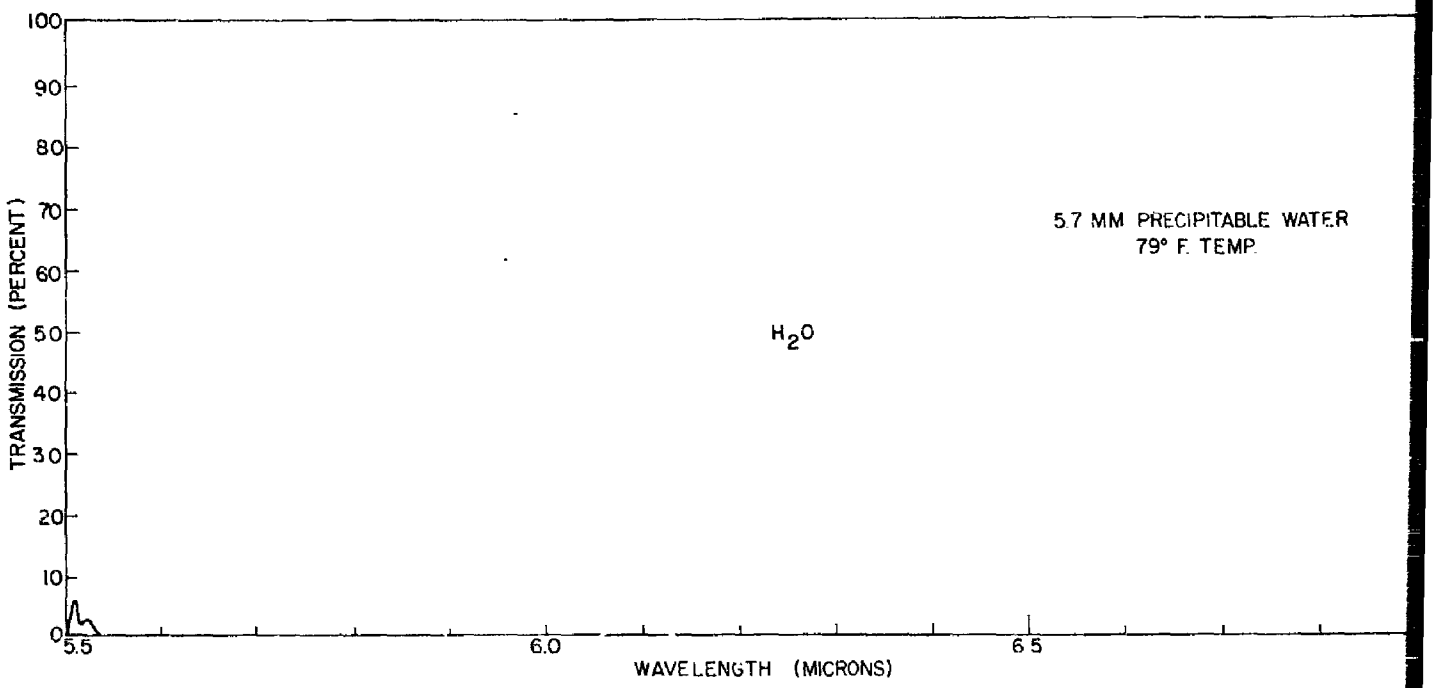

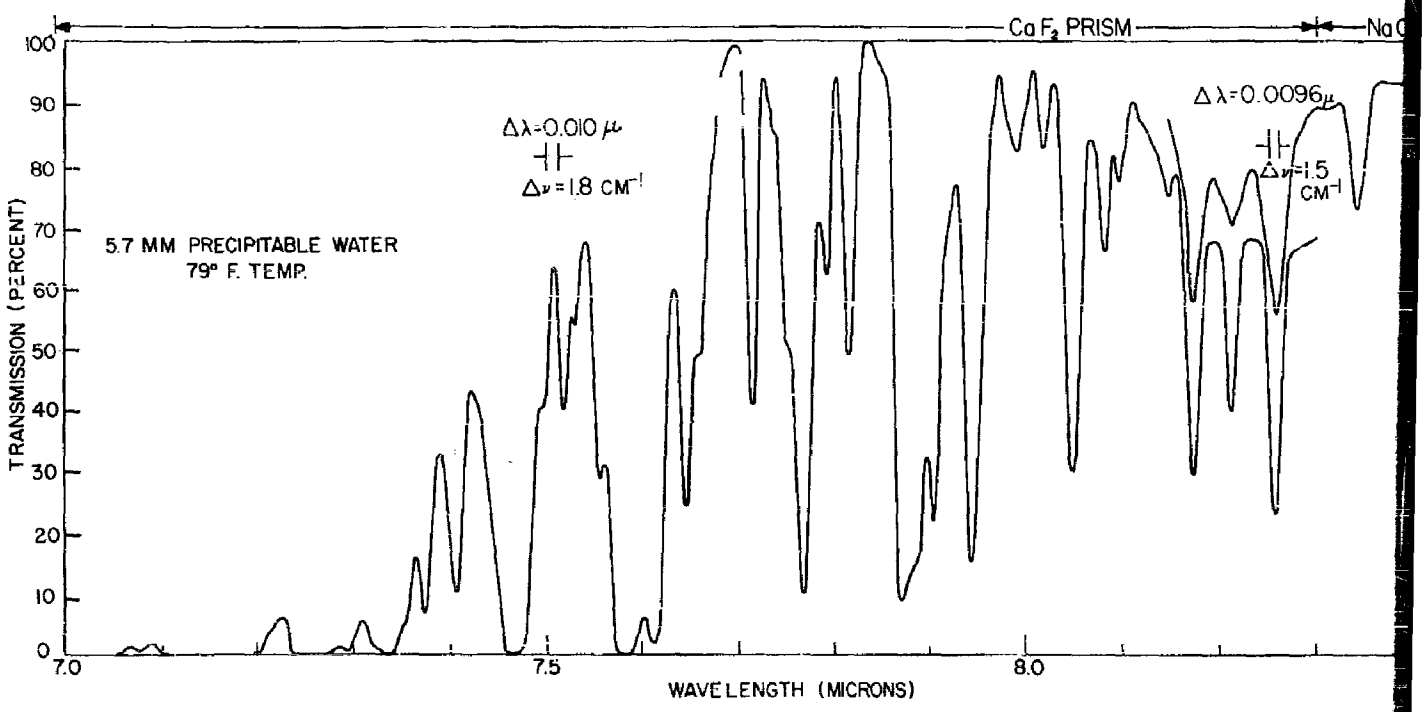

Fig. 11 (Continued) - Atmospheric transmission over a 0.3-km path in the Chesapeake Bay area. Maximum available resolution used.

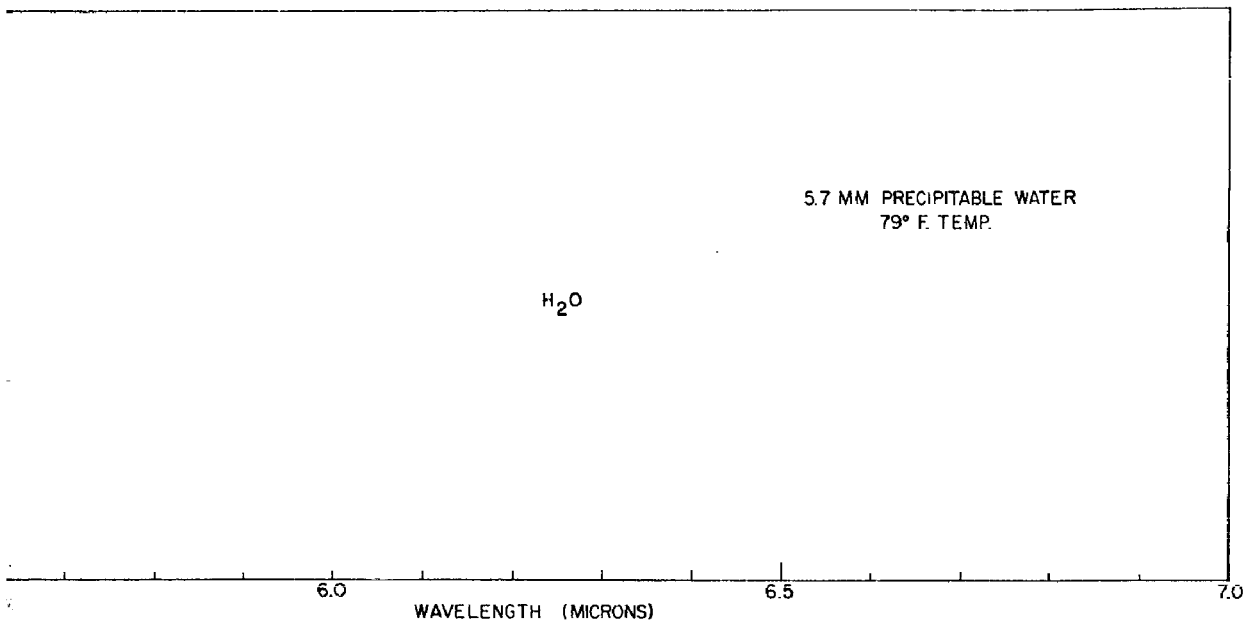

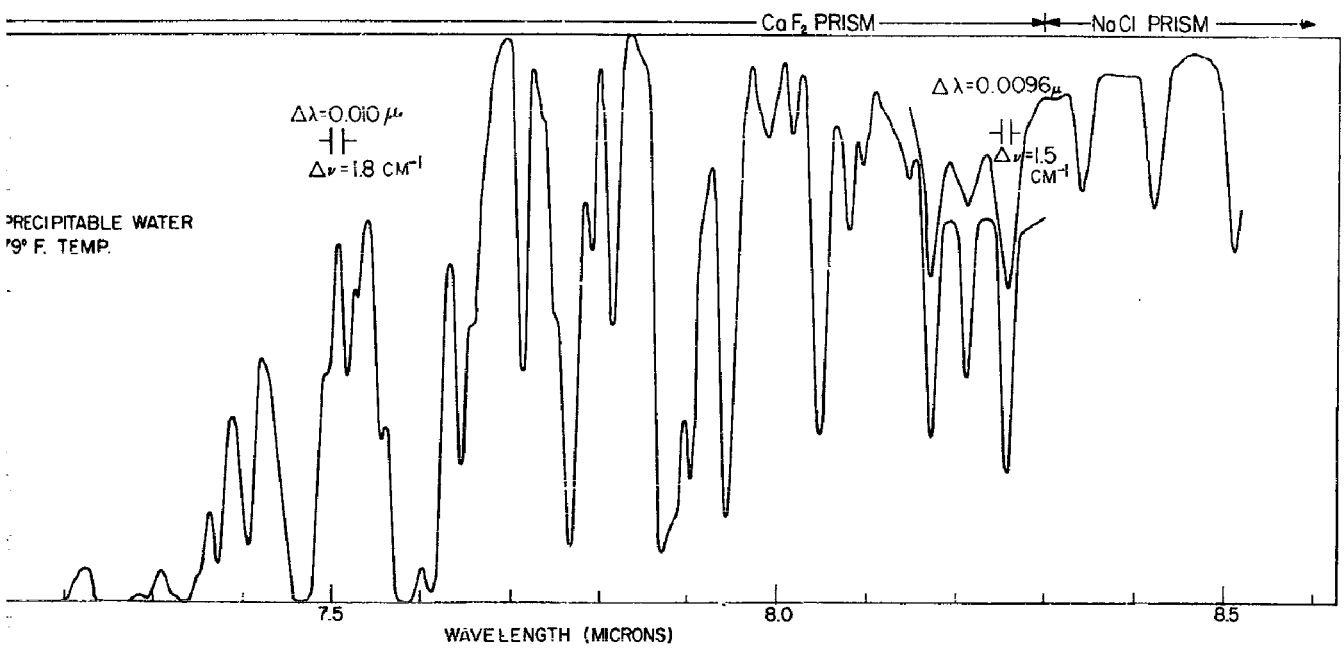

Fig. 11 (Continued) - Atmospheric transmission over a 0.3-km path in the Chesapeake Bay area. Maximum available resolution used.

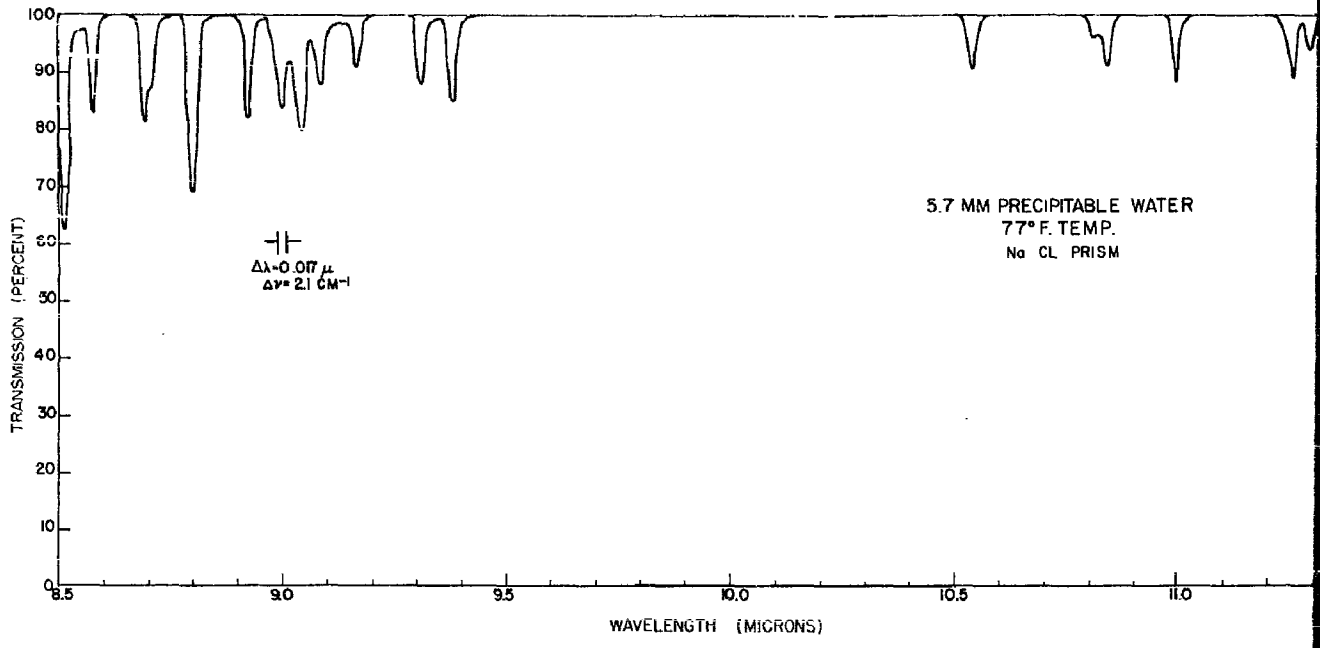

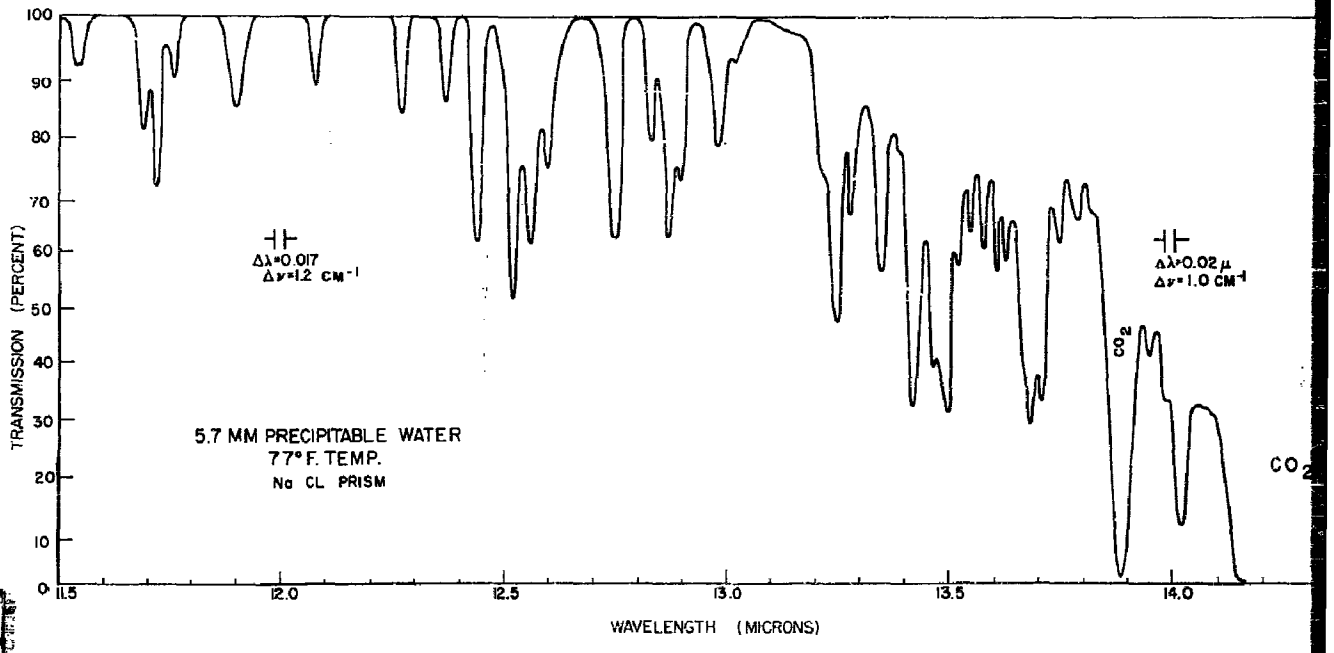

Fig. 11 (Continued) - Atmospheric transmission over a 0.3-km path in the Chesapeake Bay area. Maximum available resolution used.

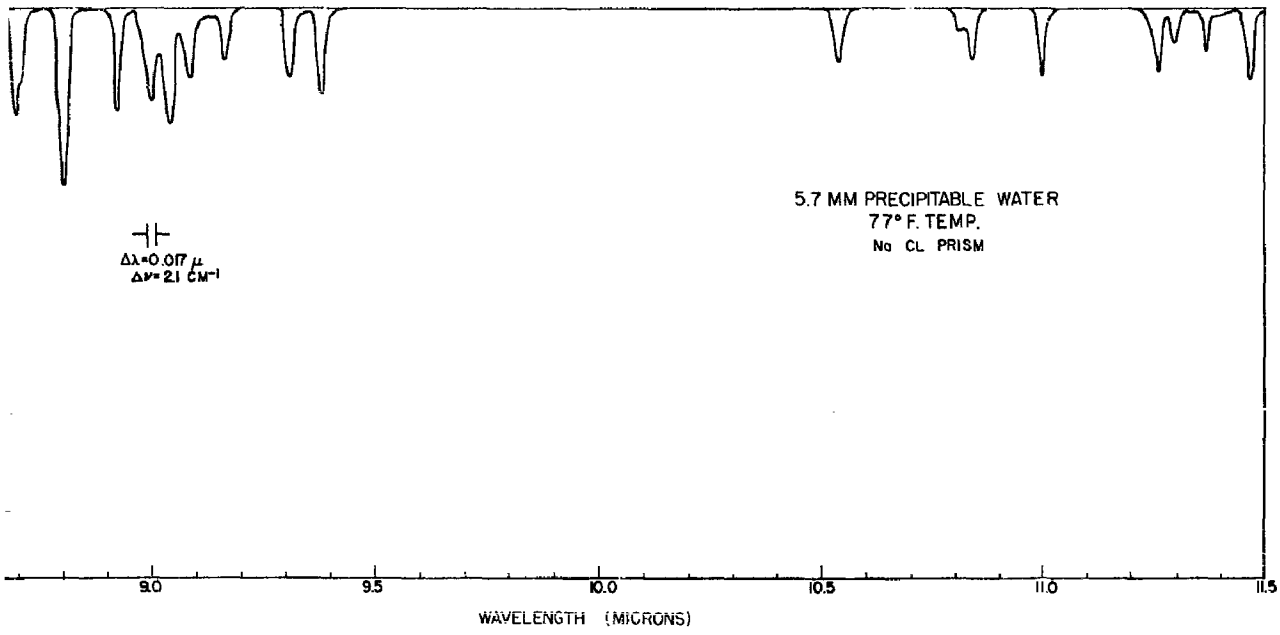

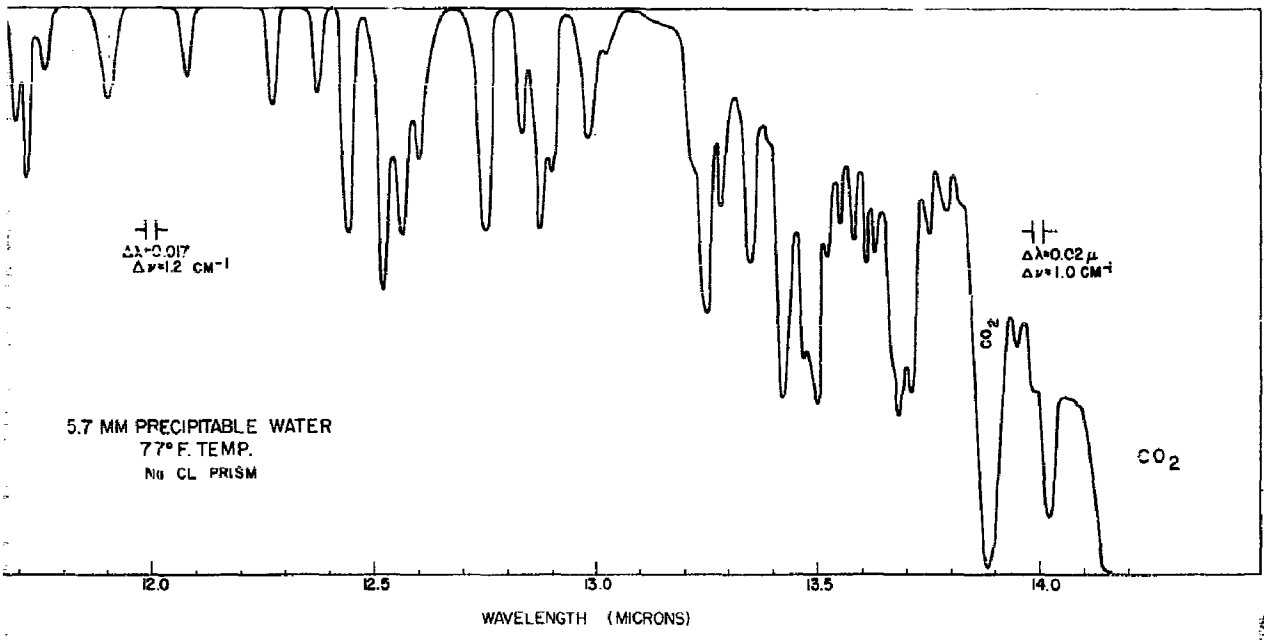

Fig. 11 (Continued) - Atmospheric transmission over a 0.3-km path in the Chesapeake Bay area. Maximum available resolution used.

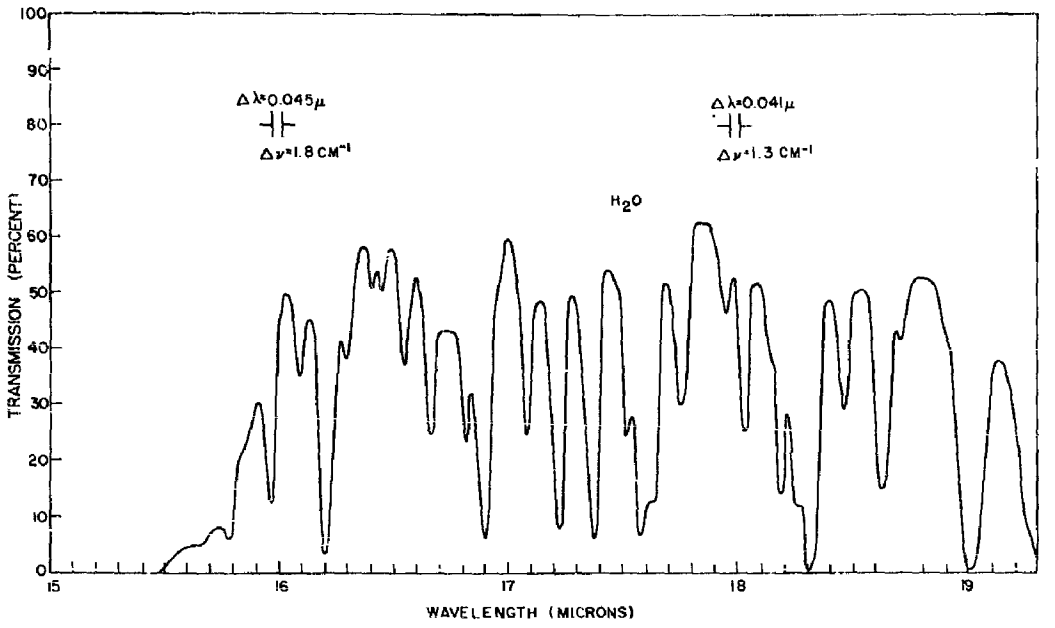

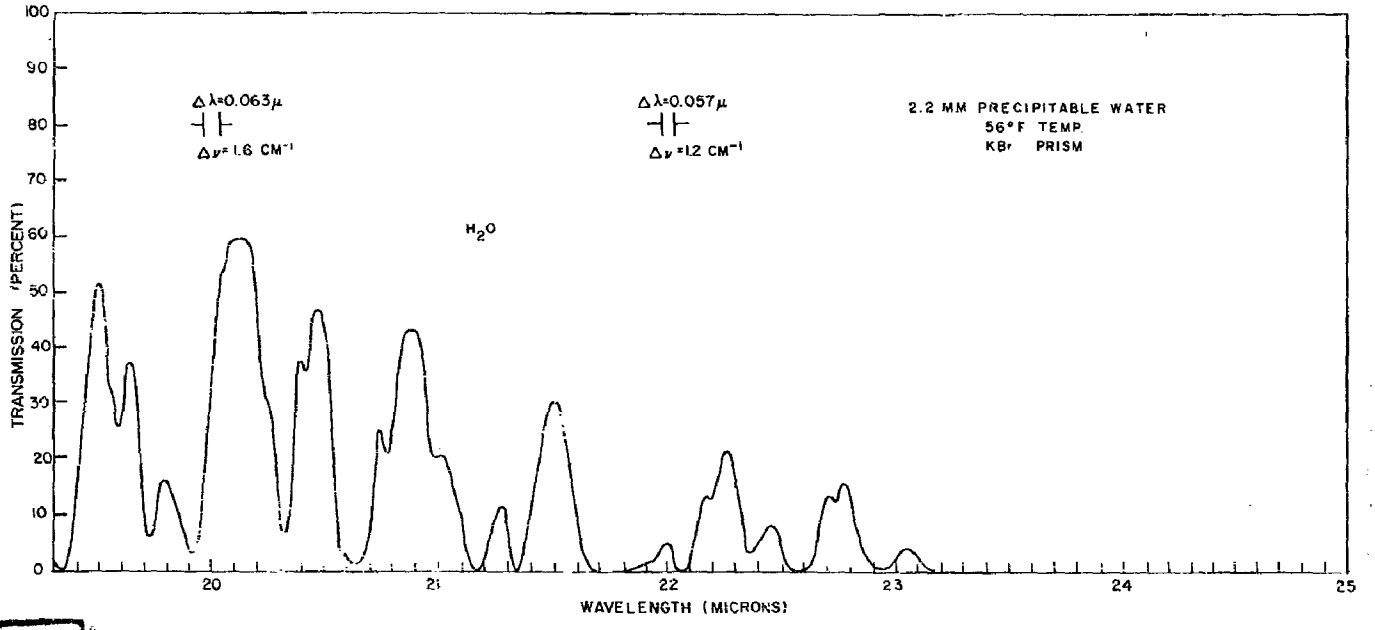

Fig. 11 (Continued) - Atmospheric transmission over a 0.3-km path in the Chesapeake Bay area. Maximum available resolution used.

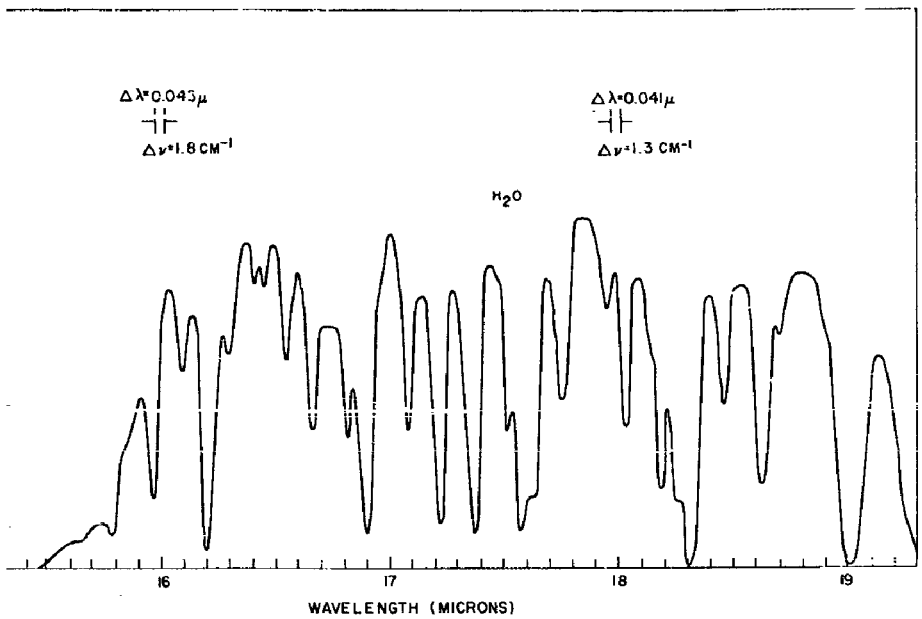

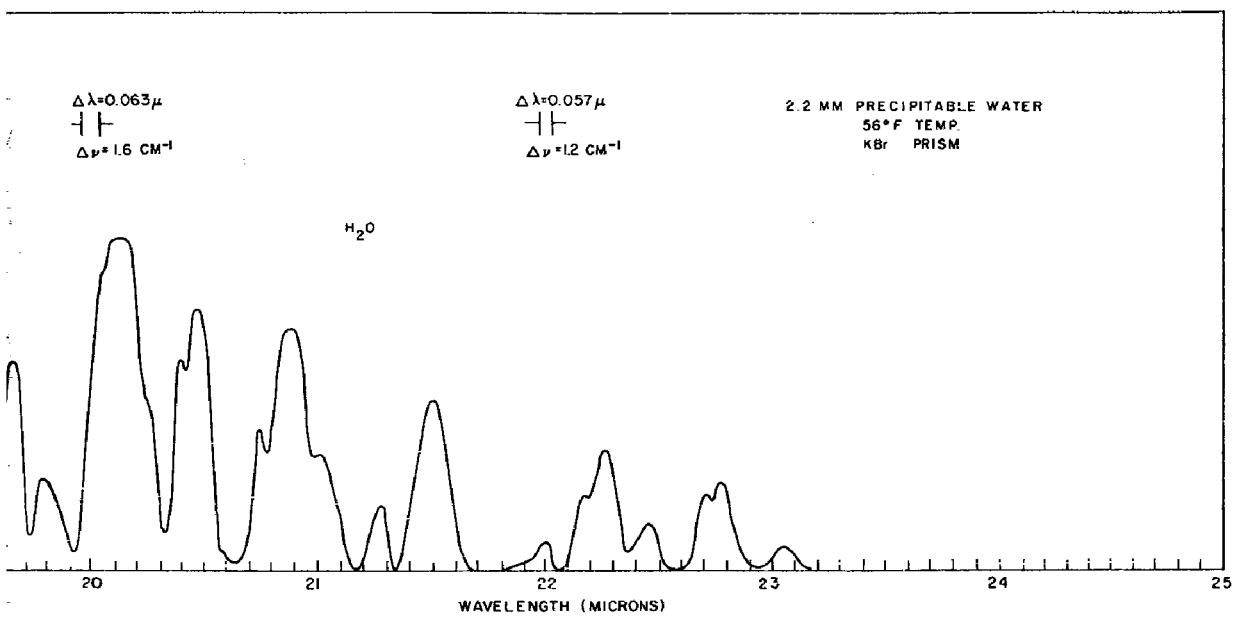

Fig. 11 (Continued) - Atmospheric transmission over a 0.3-km path in the Chesapeake Bay area. Maximum available resolution used.

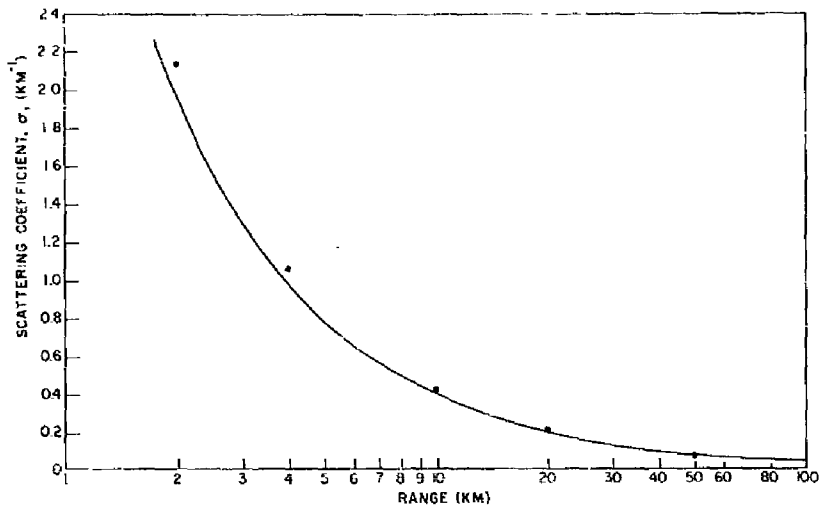

Fig. 12 - Visible scattering coefficient σ per km, as a function of range. The range is meteorological range (MR) for the solid curve, which assumes a 2-percent threshold limit. The solid points indicate visual ranges taken from the International Visibility Code.

The experimental scattering coefficients are shown in Figs. 13 through 16. In Fig. 13, four runs over the 16.25-km path are shown, ranging from a visible-region scattering coefficient of 0.24 to 0.073 km^{-1}. Figure 14 shows four additional curves for the same path and over the range 0.185 to 0.51 km^{-1} in visible-region scattering coefficient. Figure 15 shows four runs over the 5.5-km path, where σ in the visible spectrum ranges from 0.58 down to 0.065 km^{-1}.

Also plotted on Figs. 13 and 15 are typical atmospheric scattering coefficients in the 0.3 to 0.6 μ region as measured in NRL work reported by Dunkelman (17). They are included to indicate the behavior of the atmosphere in the visible and ultraviolet.

In Fig. 16 are shown the points from two runs over the 27.7-km path between the mountains in Hawaii. These two sets of points lie very close together, and one curve is drawn through them. The scattering coefficient at this relatively high altitude (one end of the path at 11,100 ft, the other at 9300 ft) is surprisingly high and, except for the occasional intervention of dense clouds, also surprisingly constant. There appeared to be an appreciable amount of scattering material lying below a fairly well defined ceiling at around 9500 to 10,000 ft. The searchlight beam, originating at 9300 ft and rising to 11,100 ft, could be seen from the side to start out bright and rather abruptly decrease in brightness. From the Weather Bureau Station at 11,100 ft, the 10,000-ft peak Haleakela on Maui (80 mi away), the mountainous Molokai (135 mi away), and the mountains on Oahu were always clearly visible when there were no intervening clouds. This would not be possible if the scattering coefficient over these high paths were as large as that measured between Mauna Loa and Mauna Kea. From Fig. 16, it will be seen that at Mauna Loa the measured value of σ at 0.55 μ was 0.05/km which, from Fig. 12, corresponds to an MR of only about 40 km. It is believed that the measured scattering coefficients would have been appreciably smaller if the source on Mauna Kea could have been moved another two thousand feet up the mountain, but the logistical problems involved in such a move were insurmountable in the present program.

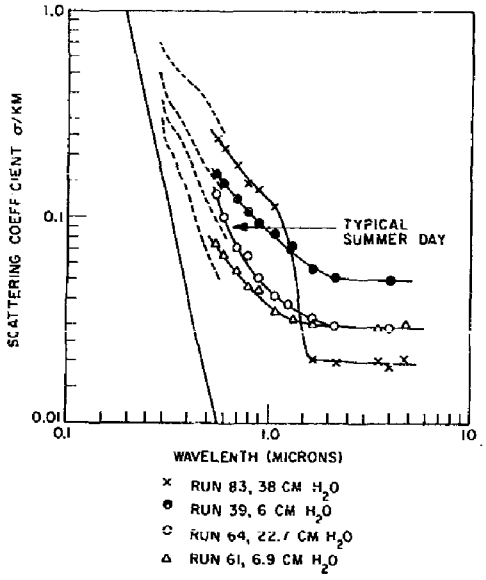

Fig. 13 - Scattering coefficient σ per km, for selected wavelength points away from absorption bands, data from measurements over 16.25 km at sea level. The dashed lines are from Table 5 of Ref. 17. The solid straight line is the Rayleigh curve for sea-level.

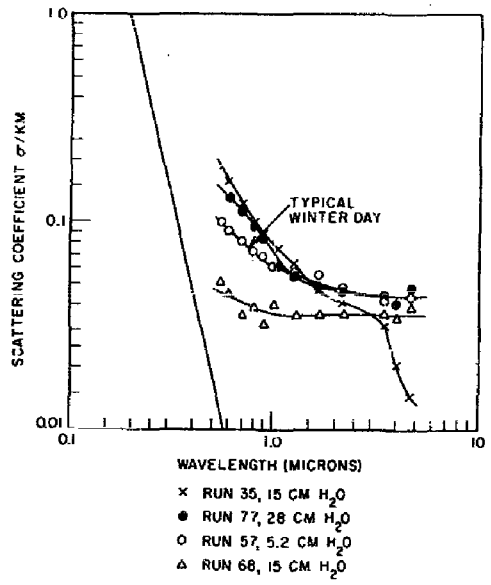

Fig. 14 - Scattering coefficient σ per km, for selected wavelength points away from absorption bands, data from measurements over 16.25 km at sea level. The solid straight line is the Rayleigh curve for sea-level air.

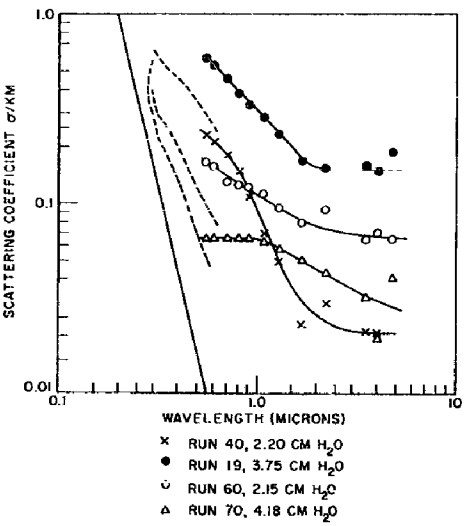

Fig. 15 - Scattering coefficient σ per km, for selected wavelength points away from absorption bands, data from measurements over 5.5 km at sea level. The dashed lines are from Table 5 of Ref. 17. The solid straight line is the Rayleigh curve for sea-level air.

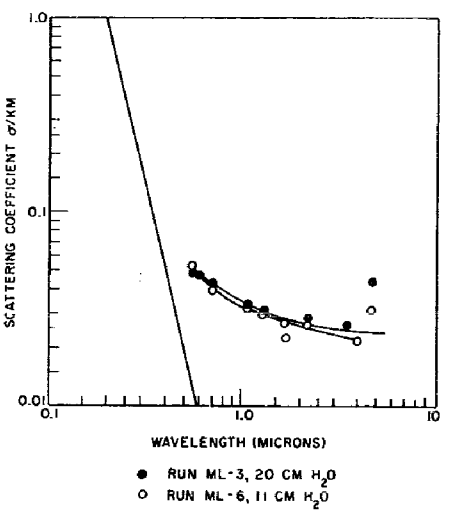

Fig. 16 - Scattering coefficient σ per km, for selected wavelength points away from absorption bands, data from measurements over 27.7-km path at 10,000-ft altitude.

For comparison, the slope of a pure Rayleigh scattering characteristic ($\sigma \sim \lambda^{-4}$) is indicated on Figs. 13 through 16. These lines are placed on the graph in a position representative of pure sea-level air devoid of any contamination such as smoke or fog. In such an atmosphere the scattering is by the molecules of O_2 and N_2.

From an examination of Figs. 13 through 16, it will be seen that the scattering coefficient in the infrared is normally about half the value in the visible region. The reduction is more pronounced for a hazier-than-average condition and less pronounced for a clearer-than-average condition. In addition, there were anomalous results (run 57 in Fig. 14 and run 40 in Fig. 15), but these were rare. The only two encountered are the two shown in Figs. 14 and 15, and there was nothing anomalous about these days, either visually or meteorologically, to aid in an explanation. It can only be construed that these days were characterized for some unknown reason by a more-than-average uniformity of particle size.

Since the present program was primarily concerned with long atmospheric paths, it was not practical to investigate highly opaque conditions such as dense fogs, rain, and snow. Through such conditions, the received radiation level was usually too low for measurement. Only two successful measurements were made in foul-weather conditions, one through a light snowstorm and one through fog mixed with light rain (12). The results of these two measurements are listed in Tables 1 and 2, where the transmission ratios between selected wavelength regions are shown. The actual transmission values fluctuated rapidly through fog and snow, making it impossible to produce a meaningful spectrum. Therefore, the spectrometer was set successively to the several discrete wavelength regions listed, and the fluctuations averaged out to produce the transmission ratios. Both runs were made over the 5.5-km path, and the slits were opened wide in order to achieve a measurable radiation level. Since the original slit program was abandoned, the actual transmission at any one point can be estimated only from signal level and is therefore probably inaccurate by a factor of as much as two to five. In the case of the snowstorm (Table 1), the transmission in the visible (0.54 μ) was estimated at 0.004 percent, and in the case of the fog (Table 2), the estimated visual transmission was 0.04 percent. The important factor to remember in looking at these tables, therefore, is that while the transmission in the infrared — around 3 to 5 μ — improved over the visible region by as much as 20 for the snow and 60 for the fog, this still results in absolute transmission values of only 0.08 percent and 2.4 percent, respectively.

Table 1
Ratio of Transmissions Over 5.5-km Path
During Snowstorm

λ_1 (microns)	λ_2 (microns)	Ratio of Transmittance at λ_1 to Transmittance at λ_2	
		Run 1	Run 2
1.26	0.54	8.9	9.0
1.54	1.26	1.58	1.63
2.18	1.54	1.06	1.2
3.98	2.18	1.15	1.46
4.69	3.98	0.77	-

Table 2
Ratio of Transmissions Over 5.5-km Path
Through Fog Mixed with Light Rain

λ_1 (microns)	λ_2 (microns)	Ratio of Transmittance at λ_1 to Transmittance at λ_2
1.04	0.54	8.14
1.21	1.04	1.45
1.59	1.21	1.45
2.27	1.59	3.0
3.64	2.27	1.25

There have been other experimental programs directly concerned with the measurement of transmission through fog and heavy weather, notably the work of Arnulf, et al., in France (18), and the reader is referred to this source for more extensive results.

SELECTIVE ABSORPTION

Introduction

The most severe atmospheric attenuation in the infrared region of the spectrum results from selective absorption by the gases in the atmosphere. Arranged in order of decreasing practical importance, these gases are water vapor, carbon dioxide, nitrous oxide, ozone, oxygen, methane, and carbon monoxide. This order differs from the order of atmospheric abundance for these gases, because some of the absorption regions overlap, and the rarer constituents may be masked by one or more of the abundant constituents. For example, methane is more abundant than nitrous oxide, but its absorption regions occur near intense water-vapor and carbon dioxide bands, so that its presence or absence is difficult to detect without very high resolving power. It contributes very little to the absorption encountered in the lower atmosphere. The relative abundance of the infrared-active gases which make up the atmosphere are listed in Table 3 (taken from Ref. 19), where their concentrations are given in atmosphere-centimeters (atmos-cm), or the thickness of a column of gas at normal temperature and pressure which is equivalent to the amount of gas contained in a vertical column of atmosphere. To compute volumetric concentrations, these numbers must be compared to the entire atmosphere equivalent, which is 8.04×10^5 atmos-cm.

Of these constituents, oxygen, carbon dioxide, nitrous oxide, and methane appear to be uniformly mixed in the atmosphere and to have stable concentrations. Water vapor, of course, is highly variable in concentration and is pronouncedly stratified. Figure 17 illustrates this large vertical gradient in water-vapor concentration, with the results of three series of measurements taken from balloon-borne instruments (20). More than 90 percent of the water vapor lies in the atmosphere below 15,000 to 20,000 ft, and it is in this region that the most pronounced changes in concentration occur. Above 20,000 ft the water-vapor concentration tends to follow the air-density curve, indicating a more nearly uniform volumetric concentration. Ozone, which absorbs appreciably in a strong band at 9.6 μ, is confined principally to a layer lying from 15 to 35 km above the earth's surface. It exerts little influence on optical paths which do not include this layer, but it

Table 3
Molecules Identified in Earth's Atmosphere*

Molecule	Molecular Weight	Atmos-Cm (NTP)
O_2	32.0	167,600
$O^{16}O^{18}$	34.0	659
$O^{12}O^{16}$	44.0	320
$O^{16}O^{17}$	33.0	134
$C^{13}O_2^{16}$	45.0	1.5
CH_4	16.0	1.2
$C^{12}O^{16}O^{18}$	46.0	0.67
N_2O	44.0	0.4
O_3	48.0	0.3
CO	28.0	0.06 - 0.15
H_2O	18.0	10^3 - 10^4
HDO	19.0	0.4 - 4.0

*Ref. 19.

is discernible in the results of the present study (21). Its concentration at sea level is only a few parts per million and is highly variable, being generally more evident by day than by night.

Atmospheric Windows

The striking feature of the infrared absorption by gases is the localization of regions of high absorption into marked bands. Generally these bands are vibration-rotation bands of the particular gas molecules. It might be mentioned that the homonuclear molecules, such as O_2 and N_2, do not have absorption bands of this type. The near-infrared O_2 absorption structure (0.78 μ) corresponds to an electronic transition.

As can be seen from any of the spectra in Figs. 5 through 11, the selective absorption bands are scattered through the infrared spectrum. Between the absorption bands lie regions of moderate or no selective absorption. These regions of relatively good transmission have been named "atmospheric windows" and have the generally accepted definitions listed in Table 4.

In specifying the transmission of an optical path at wavelengths which cover atmospheric windows, a very useful quantity is the "selective-window transmission." This concept was first introduced by Elder and Strong (22) and has become widely used. The selective-window transmission for a given window is defined as the ratio of the energy that actually penetrates the atmosphere between the wavelength limits of the window,

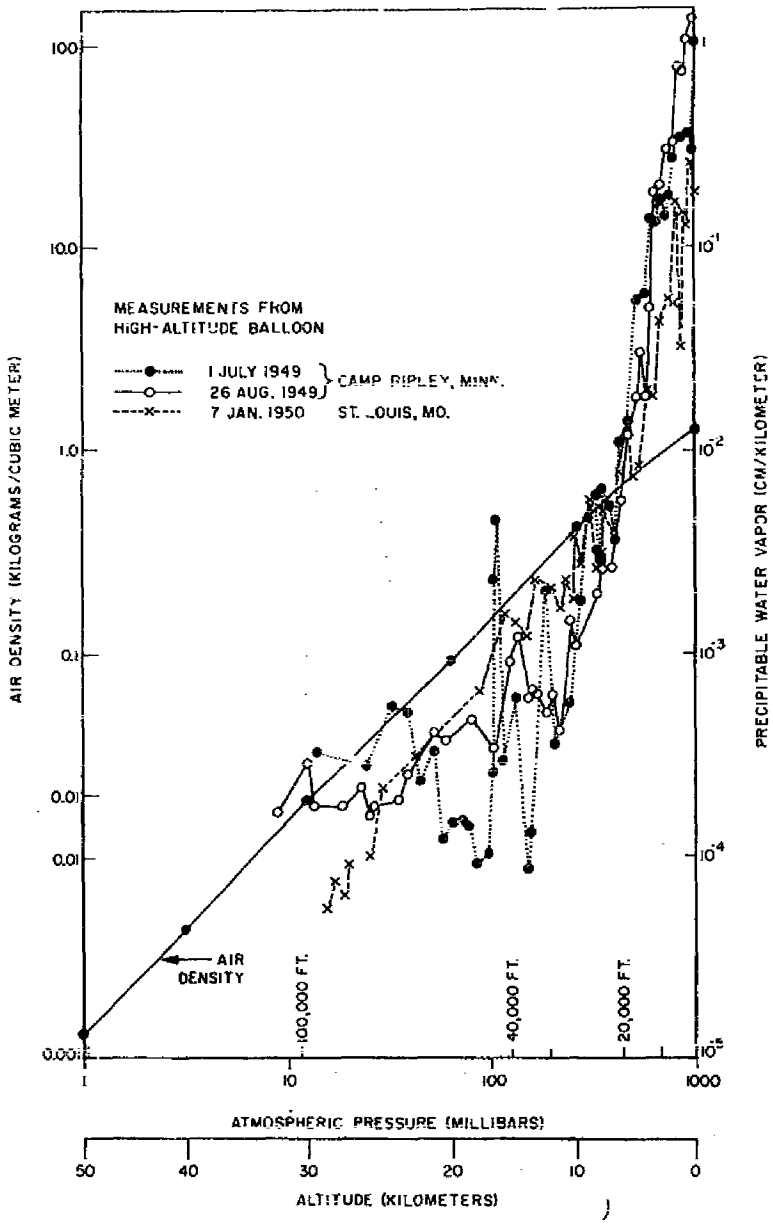

Fig. 17 - Examples of the vertical distribution of water vapor, data from Ref. 20

Table 4
Atmospheric Window Definition

Window Number	Wavelength Limits (microns)
I	0.72 to 0.94
II	0.94 to 1.13
III	1.13 to 1.38
IV	1.38 to 1.90
V	1.90 to 2.70
VI	2.70 to 4.30
VII	4.30 to 6.00
VIII	6.0 to 15.00
IX	15.0 to 25.0

divided by the energy that would be received in the absence of any selective absorbers. The selective-window transmission then accounts for only selective absorption and does not take into consideration scattering losses.

As part of the present program, an effort was made to obtain selective-window transmission as a function of water-vapor concentration, in order to extend the data available in Ref. 22.

Experimental Results

Figures 18 through 24 show the selective-window transmission for windows II through VIII plotted as a function of the precipitable water vapor in the path for a broad cross section of the results obtained in this program. Window I has been omitted because of its very slight dependence on water vapor concentration and window IX because it becomes essentially opaque through only 5 or 6 mm of water vapor. Figure 25 illustrates the apparent precipitable water in the Hawaiian path vs time as measured by the absolute humidity on Mauna Loa and Mauna Kea. These values, which apply to the time during which the data in Fig. 10 were being collected, emphasize the need for continuous measurement during data runs.

In each of Figs. 18 through 23, the slope of the appropriate curve from Elder and Strong's report (22) has been reproduced as a dashed line. The points from the present study have also been identified as to the individual path — 0.3, 5.5, 16.25, or 27.7 km — over which the result was obtained. The points for the different paths will be seen to fall on different straight lines, almost all of which lie slightly below the lines extrapolated from Ref. 22.

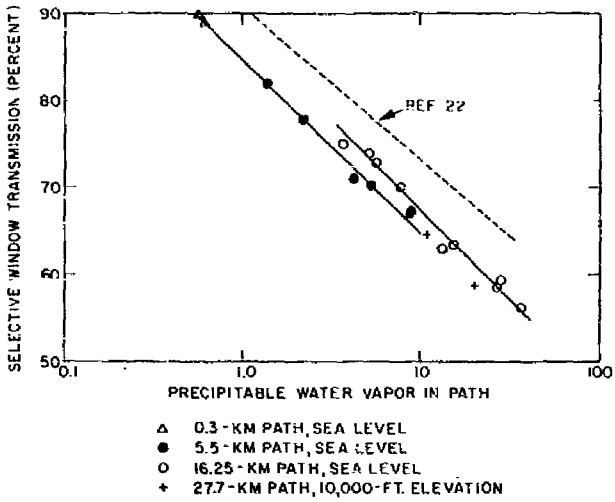

Fig. 18 - Selective transmission of Window II (0.94 to 1.13 μ) as a function of precipitable water in the path

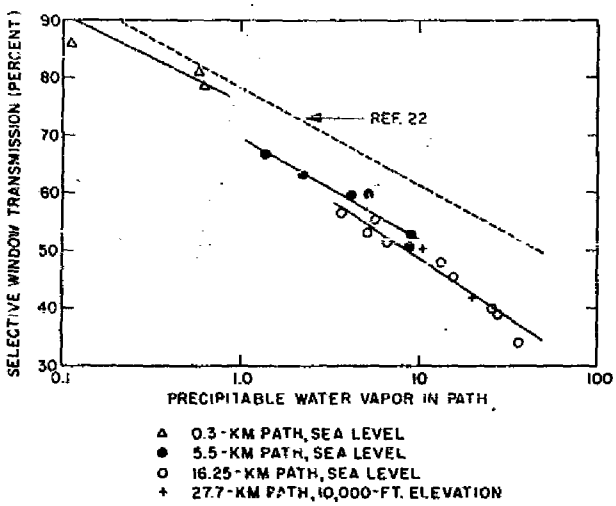

Fig. 19 - Selective transmission of Window III (1.13 to 1.38 μ) as a function of precipitable water in the path

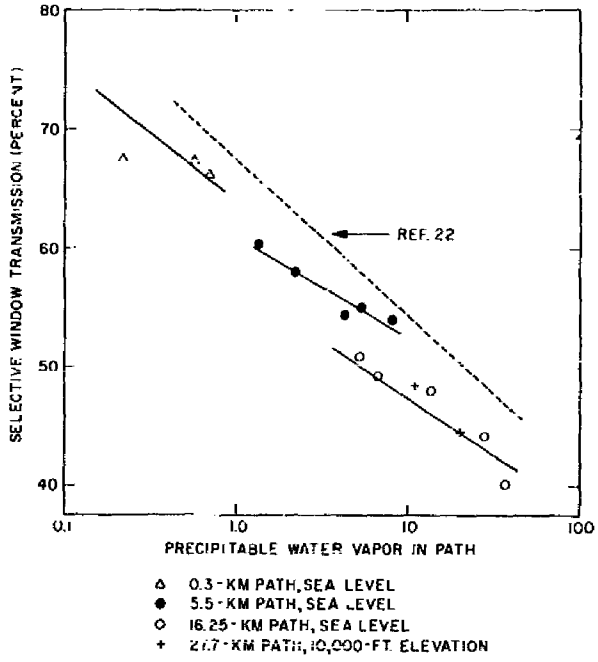

Fig. 20 - Selective transmission of Window IV (1.38 to 1.90 μ) as a function of precipitable water in the path

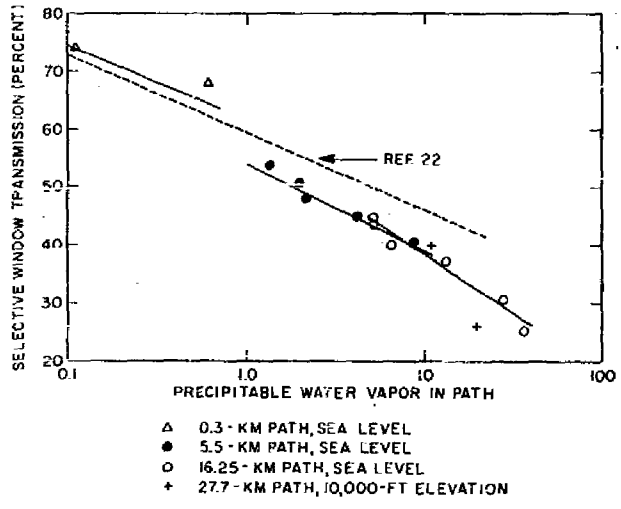

Fig. 21 - Selective transmission of Window V (1.90 to 2.70 μ) as a function of precipitable water in the path

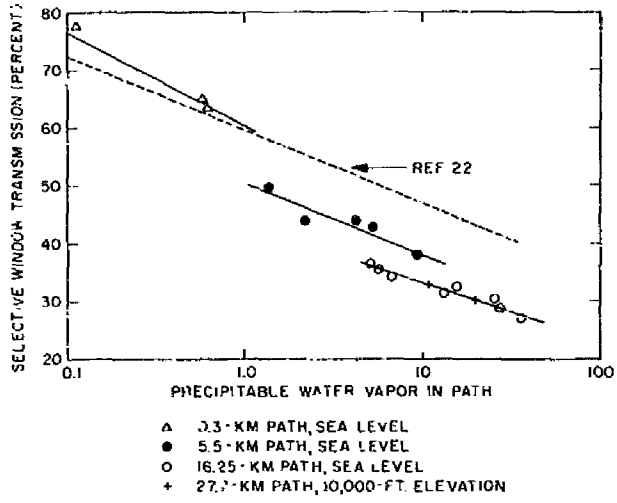

Fig. 22 - Selective transmission of Window VI (2.7 to 4.3 μ) as a function of precipitable water in the path

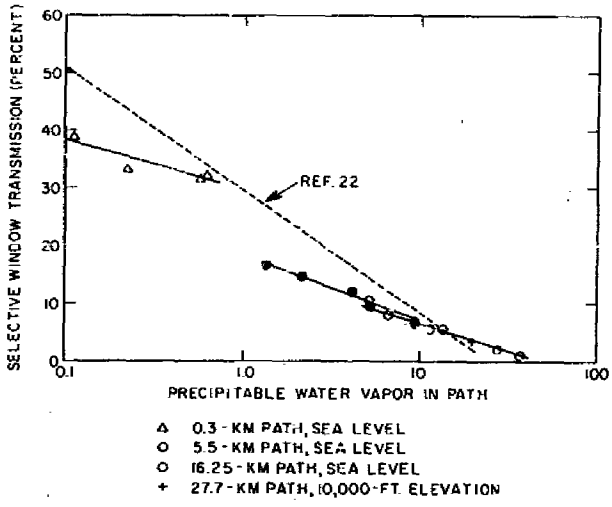

Fig. 23 - Selective transmission of Window VII (4.3 to 6.0 μ) as a function of precipitable water in the path

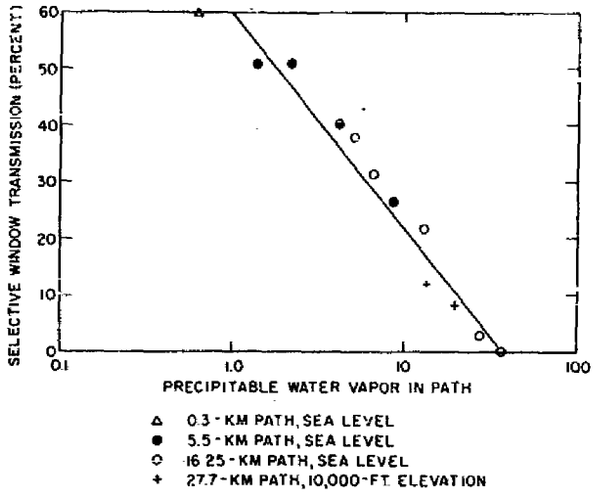

Fig. 24 - Selective transmission of Window VIII (6.0 to 15 μ) as a function of precipitable water in the path

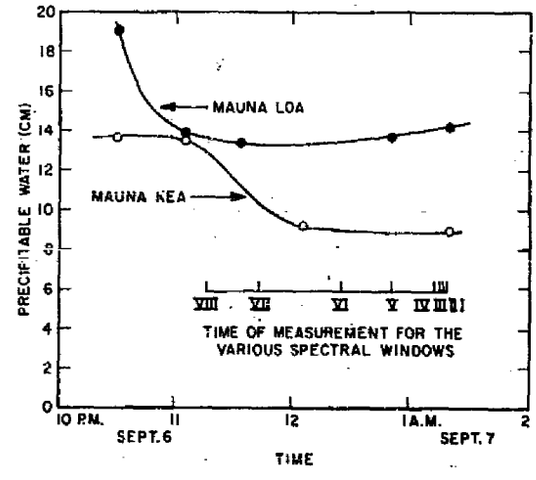

Fig. 25 - Precipitable water vapor in the Hawaiian path as a function of time computed from observations at Mauna Loa and Mauna Kea. These conditions prevailed during run ML-6 (Fig. 10).

This separation of lines with path length indicates that the transmission of an atmosphere containing a fixed number of water molecules is not a function of the precipitable water alone. There are two phenomena which would give rise to this type of effect, and it is probable that both are present in these data.

The first phenomenon is that of pressure broadening, which results in an increase in the absorption of a fixed quantity of gaseous absorber as the total pressure of the gas increases. In this phenomenon it happens that self-broadening, or the effect of absorber molecules, is greater than foreign-gas broadening, or the effect of unlike molecules. Therefore, for a fixed total pressure and a fixed quantity of absorber, the absorption will increase with the partial pressure of the absorber. This would be manifested as a higher window transmission when a fixed amount of absorber is spread out over a longer path. In Figs. 18 through 23, the short-path points should fall below the long-path points if this phenomenon is present.

The second phenomenon is the presence of absorption due to atmospheric constituents other than water. The effect of these constituents, which generally have uniform concentrations and exist in any optical path in a quantity proportional to path lengths, is to produce greater absorption in the longer paths. For this effect, the long-path points in Figs. 18 through 23 would lie below those of shorter paths.

Window II, Fig. 18, whose selective window transmission is almost completely dependent upon water vapor (it contains one weak oxygen band), is seen to follow the pressure-dependence pattern, since the points for the 16.25-km path lie above those for the 0.3- and 5.5-km paths. It is surprising to observe, however, that the points from the 27.7-km path, which should show even higher transmission, because this lower pressure path lies at an elevation of 10,000 ft, lie more nearly on the 5.5-km curve. There is no immediate explanation for this anomaly.

Window III, which contains only one moderate oxygen line, should be similar to Window II, but it shows a strong separation of lines characteristic of the presence of appreciable absorption due to constituents other than water vapor. There is no immediate explanation for this.

Window IV, which embraces some weak absorption bands of CO_2 and CH_4, shows a very pronounced separation of the lines — rather surprisingly large — and a more shallow slope than the Elder and Strong curve. It is interesting to note, however, that a single line drawn through all the points would have a slope similar to that from Elder and Strong.

Window V contains a large number of moderately strong lines of CO_2 and some very weak ones due to CH_4 and N_2O. It shows a pronounced separation between the 0.3-km and 5.5-km paths but not between the 5.5-km and longer paths.

Window VI is bounded on one edge by a very strong CO_2 band and contains considerable absorption due to weaker CO_2 bands and moderately strong bands of N_2O, CH_4, and CO. It shows the most pronounced separation of lines of all the windows except for the fact that the 27.7-km path falls on the 16.25-km path as it tends to do in almost all the windows. It is probable that the effect of absorption by constituents other than water vapor is partially offset by the slight increase in transmission due to the reduced atmospheric pressure in this path, the two effects working against one another.

Window VII contains very strong CO_2 absorption and some very weak O_3 and CO absorption. The line separation is quite pronounced, although between the longer paths it is not so obvious because the transmission is so low. This window is almost completely opaque through 40 cm of water vapor.

Window VIII is bounded by a strong CO_2 band and contains absorption by O_3, N_2O, and CH_4 but shows no tendency for separation of the paths. It is probable that it goes to zero too rapidly for the effect to be manifest with the accuracy of the present study. Over the 16.25-km path (Fig. 8), through 38 cm of water vapor, no radiation could be measured from the source, indicating a transmission everywhere less than 0.5 percent in the window.

ACKNOWLEDGMENTS

The authors wish to express their gratitude and appreciation to the many people whose efforts have contributed either directly or indirectly to the success of this experimental program. To Dr. L.F. Drummeter, many thanks for patient guidance, and to Mr. Thomas Cosden, our appreciation for his persistent and effective efforts to keep the equipment running whatever the time, location, or conditions. Mr. Lloyd Knestrick contributed to the experimental program and the data analysis, and Mr. Joseph Curcio filled in when the field team was reduced by illness.

The operation in the mountains of Hawaii would hardly have been possible without the generous assistance of the Hawaii National Guard and, in particular, Col. Michael Roman and his unit. In the difficult tasks of moving and installing heavy equipment at high altitudes and in rough terrain, Major John D'Arujio and his men frequently exceeded the requirements of their normal duties. The spirit and proficiency of this National Guard Unit are exemplary.

The cooperation of the Weather Bureau in freely making available the facilities of their new station on Mauna Loa materially aided this program. Mr. Roy Fox of the Honolulu office and Mr. Jack Pales, head of the Mauna Loa Observatory, did everything within their capabilities to assist the program. Their efforts are most gratefully acknowledged.

REFERENCES

1. Fowle, F.E., "Smithsonian Miscellaneous Collections," Vol. 68, No. 8 (1917)

2. Fischer, Heinz, "The Influence of the Spectral Transmission of Optics and the Atmosphere on the Sensitivity of Infrared Detectors," USAF Technical Report F-TR-2104-ND, Oct. 1946

3. Strong, J.D., "Atmospheric Attenuation of Infrared Radiation," OSRD Report 5986, Nov. 30, 1945

4. Gebbie, H.A., Harding, W.R., Hilsum, C., Pryce, A.W., and Roberts, V., "Atmospheric Transmission in the 1 to 14 Micron Region," Great Britain A.R.L./R.4/E-600, Dec. 1949, also Proc. Roy. Soc. A. 206:87 (1951)

5. Benesch, W., Elder, T., and Strong, J., "Absorption Spectrum of the Lower Atmosphere from 2.5 to 4.0 Microns," Progress Report on ONR Contract N5-ori-16605, Johns Hopkins U., Sept. 15, 1950

6. Migeotte, M., Neven, L., and Swensson, J., "The Solar Spectrum from 2.8 to 23.7 Microns, Part I: Photometric Atlas, Part II: Measures and Identifications," U. of Liege Final Reports Contract AF61 (514) - 432, 1957

7. Mohler, O.C., Pierce, A.K., McMath, R.R., and Goldberg, L., "Photometric Atlas of the Near Infra-Red Solar Spectrum, λ8, 465 to λ25, 242," U. of Michigan Press, Ann Arbor, 1950

8. Talbert, W.W., Templin, H.A., and Morrison, R.E., "Quantitative Solar Spectral Measurements at Mt. Chacaltaya (17,000 ft)," paper presented at Eastern Section IRIS, NOL, 5th meeting, Feb. 3, 1958

9. Benesch, W., Strong, J., and Benedict, W.S., "The Solar Spectrum from 3.3 to 4.2 Microns," Progress Report on ONR Contract N5-ori-16605, Johns Hopkins U., Aug. 1, 1950

10. Howard, J.N., Burch, D.L., and Williams, D., "Near Infrared Transmission through Synthetic Atmospheres," AFCRC-TR-55-213 Geophysical Research Papers No. 40, Geophysics Research Directorate, AFCRC, Air Research and Development Command, Nov. 1955

11. Drummeter, L.F., Jr., "The Infrared Absorption of Water Vapor at 1.8 Microns," Thesis, Johns Hopkins U., 1949

12. Taylor, J.H., and Yates, H.W., "Atmospheric Transmission in the Infrared," NRL Report 4759, July 2, 1956, also J. Opt. Soc. Am. 47(3):223 (1957)

13. Yates, H.W., "The Absorption Spectrum from 0.5 to 25 Microns of a 1900-Foot Atmospheric Path at Sea Level," NRL Report 5033, Sept. 1957

14. Goldstein, E., "The Measurement of Fluctuating Radiation Components in the Sky and Atmosphere - Part II," NRL Report 3710, July 1950

15. Downie, A.R., Magoon, M.C., Purcell, T., and Crawford, B., Jr., "The C[illegible] of Infrared Prism Spectrometers," J. Opt. Soc. Am. 43(11):941 (19[illegible])

16. Cosden, T.H., "Recording Horizontal Atmospheric Transmission of Li[illegible] and Day," NRL Report 4570, July 1955

17. Dunkelman, L., "Horizontal Attenuation of Ultraviolet and Visible Light [illegible] Lower Atmosphere," NRL Report 4031, Sept. 1952

18. Arnulf, A., Bricard, J., Curé, E., and Véret, C., "Transmission [illegible] in the Spectral Region 0.35 to 10 Microns," J. Opt. Soc. Am. 47(6):[illegible]

19. Goldberg, L., "Infrared Solar Spectrum," Am. J. Phys. 23(4):203 (1955)

20. Barnett, E.A., Herndon, L.R., Jr., and Carter, H.J., "Some Measurements [illegible] Distribution of Water Vapor in the Stratosphere," Tellus 7:302 (1955)

21. Taylor, J.H., and Yates, H.W., "Infrared Emission for Atmospheric Ozone Layer," letter to editor, J. Opt. Soc. Am. 47(11):998 (1956)

22. Elder, T., and Strong, J., "The Infrared Transmission of Atmospheric [illegible] Bulletin [illegible] (1953)

* * *

Recd 11/21/2000

Naval Research Laboratory
Technical Library
Research Reports Section

DATE: October 24, 2000

FROM: Mary Templeman, Code 5227

TO: **Code 5600 Dr Giallorenzi**

CC: Tina Smallwood, Code 1221.1 ts 10/30/00

SUBJ: Review of NRL Reports

Dear Sir/Madam:

1. Please review NRL Report 5453 for:

   ☑ Possible Distribution Statement
   ☐ Possible Change in Classification

Thank you,

Mary Templeman
(202)767-3425
maryt@library.nrl.navy.mil

The subject report can be:

☑ Changed to Distribution A (Unlimited)
☐ Changed to Classification _____
☐ Other:

[signature] 10/25/00
Signature Date